UNIVERSITÀ DEGLI STUDI DI PADOVA

Dipartimento di Fisica e Astronomia “Galileo Galilei”

Master’s degree in physics

Final Dissertation

Influence of moisture transport on the predictability of Mediterranean cyclones: a dynamical systems perspective

Thesis supervisor

Prof. Francesco Marra

Thesis co-supervisor

Prof. Cinzia Sada

Candidate

Moreno Mencato

Academic Year 2025/2026

Contents

Introduction

Accurate forecasting of extreme weather conditions is typically achieved through numerical simulations of the atmosphere. Recent developments in dynamical systems theory allow atmospheric states to be described in terms of two metrics, their persistence θ^{-1} and local dimension d, this approach provides information on how the atmosphere will evolve in the proximity of a given state of interest. These metrics are intuitively linked to the intrinsic predictability of the atmosphere: a highly persistent, low-dimensional state will be, intrinsically, more predictable than a low-persistence, high-dimensional one.

It is known that moisture absorption influences the predictability of Mediterranean cyclones, but little is known about the potential influence of moisture transport. The objective of this thesis is to identify and quantify the possible influence of moisture transport on the intrinsic predictability of Mediterranean cyclones, in the eastern Mediterranean. Moisture transport is quantified using a vector quantity called Integrated Vapor Transport (IVT), defined as the horizontal advection of vapor integrated vertically along the vertical tropospheric column.

The Mediterranean has been recognized as one of the regions which is currently being affected by climate change and is predicted to be influenced in the future by warning and drying and, at the same time, by an intensification of the extreme precipitation events. Among the unique characteristics of the Mediterranean region is the coexistence of different kinds of cyclones. In fact, despite their generally limited size and duration, Mediterranean cyclones are known to have a significant impact on the highly populated coastal areas around the basin, due to the strong winds and heavy rainfall that accompany them. This explains why the study of extreme weather events, in addition to its theoretical importance, is also of considerable social and economic significance.

The thesis is organized as follows: Chapter 1 offers a general description of the Earth's atmosphere, focusing on its main thermodynamic and dynamic properties. The second chapter discusses some characteristics of dynamic systems, with particular attention to attractors, which we can define as a set of states towards which the system tends to evolve in the long term, regardless of the initial conditions, within a certain region of space. Measures of the intrinsic predictability of a dynamic system are the provided, by first introducing Lyapunov exponents, and then arriving to a formal definition of the local dimension d and persistence θ^{-1}. The third chapter, the data provided will be analysed. The data consists of two lists, one containing the cyclones that occurred in the area of interest, another containing the values of the metrics d and θ for each day, and a third source consisting of the IVT values downloaded from the ERA5 database. By comparing the data provided, we investigate whether an increase in moisture transport can influence the intrinsic predictability of the atmospheric system, i.e. whether such an increase leads to a variation in the metrics d and θ. We found that greater moisture transport would seem to lead to a decrease in the value of the local metric d for the geopotential height Z1000 (i.e., near the ground) for the most intense cyclones, thus indicating a possible increase in intrinsic predictability. As regards the θ metric, no results were obtained that indicated a possible influence of moisture transport on the inverse of persistence θ.

Chapter 1

Earth’s atmosphere

The purpose of this first chapter is to provide a brief introduction to some general properties of the Earth's atmosphere. We will then proceed to describe some fundamental aspects of thermodynamics and atmospheric dynamics.

1.1 Constituents and vertical structure

The atmosphere of the Earth is a vast expanse of gases enveloping the planet. Within this envelope, we are surviving and all our activities are confined. It is made up of several gases (Figure 1.1), water vapour and minute particles suspended in the gaseous substance of air. The four major gases: nitrogen, oxygen, argon and carbon dioxide together constitute 99.99% of the total volume of dry air. The maximum concentration is of nitrogen with more than 78 percent while the oxygen is little less than 21 percent. Water vapor, which accounts for roughly 0.25% of the mass of the atmosphere is a highly variable constituent, with concentration ranging from around 10 parts per million by volume in the coldest region of Earth’s atmosphere up to as much as 5% by volume in hot, humid air masses.

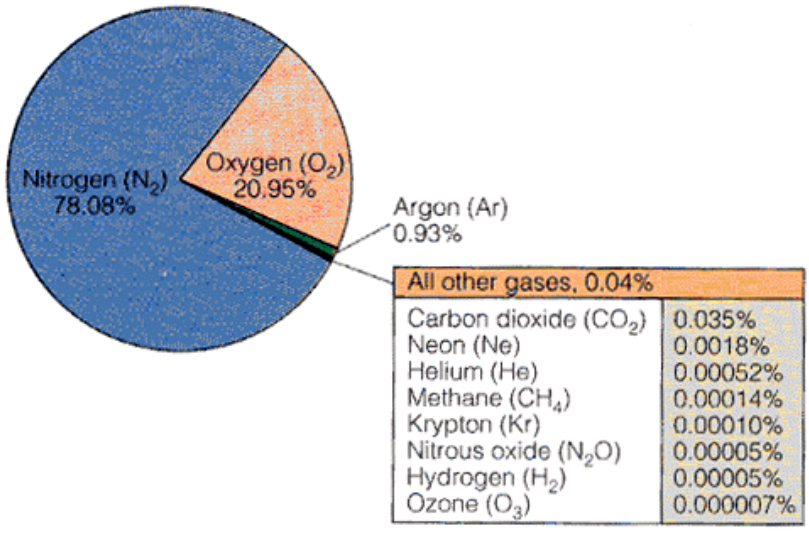

Figure 1.1-Composition of the dry air in volume percent. (From Air Pollution and control, Dr. Tanushree Bhattacharya, BIT Mesra, 2024.)

Gaseous particles forming the atmosphere are prevented to fly away by the gravitational attraction which the planet exerts on them. Gravitational force is in fact the main responsible for the

atmosphere's structure, stratifying mass vertically. This stratification of mass results in a strong kinetic constraint on atmospheric motion: vertical displacements of air result to be much smaller than horizontal ones if circulations spanning a few tens of kilometres in the horizontal direction are considered. Vertical and horizontal displacements are comparable only when considering small-scale.

The pressure p and the density ρ decrease nearly exponentially with height:

$$p = p_0 e^{-z/H} \quad \text{or equivalently} \quad \ln \frac{\mathrm{p}}{\mathrm{p_0}} = -\frac{z}{H} \tag{1.1}$$

where H is called *scale height* and p_0 is the pressure at some reference level, which is usually taken at sea level (z=0). In the lowest 100 km, the scale height ranges roughly from 7 to 8 km.

Density decreases with height in the same way as pressure. These variations in pressure and density with height are much greater than the corresponding horizontal and temporal variations, so it is useful to define an idealized representation of the structure of the atmosphere, a standard atmosphere that represents the horizontal and temporal average of the structure of the atmosphere as a function of height alone.

Based on its chemical composition, the atmosphere can be classified into two parts. They are homosphere and heterosphere. Homosphere is that part of atmosphere where the chemical composition of the air tends to be quite uniform and independent of height due to mixing by turbulent fluid motion. It is the lowest layer in terms of chemical composition. It extends from the earth's ocean surface to about 85 km. Above ~100 km , where the mean free path between molecular collisions exceeds 1m, individual molecules species are sufficiently mobile that each molecular species behaves as if it alone were present. Under these conditions, the concentrations of heavier constituents decrease more rapidly with height than those of lighter constituents. Indeed, the density of each constituent drops off exponentially with height, but as it is possible to see, with a scale height *H* inversely proportional to the molecular weight. The upper layer of the atmosphere in which the lighter molecular species become increasingly abundant (in a relative sense) with increasing height is referred to as the heterosphere. The upper limit of the lower layer of the atmosphere, in which constituents result to be well-mixed, is called turbopause, where turbo refers to turbulent fluid motions. The composition of the outermost reaches of the atmosphere is dominated by the lightest molecular species (H, He, and H_2).

Considering the variation in temperature with altitude, we can divide the atmosphere into four layers: *troposphere*, s*tratosphere*, *mesosphere* and *thermosphere* (Figure 1.2). Troposphere is the lowest and densest of these layers. Approximately 80 per cent of the total mass of the atmosphere lies within it. As altitude increases, the temperature tends to decrease at a rate that is approximately constant,

$$\Gamma \equiv \frac{\partial \mathrm{T}}{\partial \mathrm{z}} \sim 6.5^{o}\mathrm{C\ km^{-1}} \tag{1.2}$$

where T is the temperature, z is the height and Γ is the lapse rate. Water vapour is found in this layer in abundance and about 99 percent of the total atmospheric water vapour is concentrated here but wide spatial and temporal variations are seen in concentration. All weather phenomena are occurring in this layer only. Troposphere is the home of all types of clouds, atmospheric turbulence and mixing of the air. The upper boundary of the troposphere, called tropopause, is identified by a clear change of the temperature profile, which shifts from decreasing to increasing with height. From an altimetric point of view, the tropopause generally extends from approximately 8 to 17 kilometres above the Earth's surface, varying according to latitude, season and local atmospheric conditions. Its location is influenced by various factors, including the temperature and chemical composition of the atmosphere.

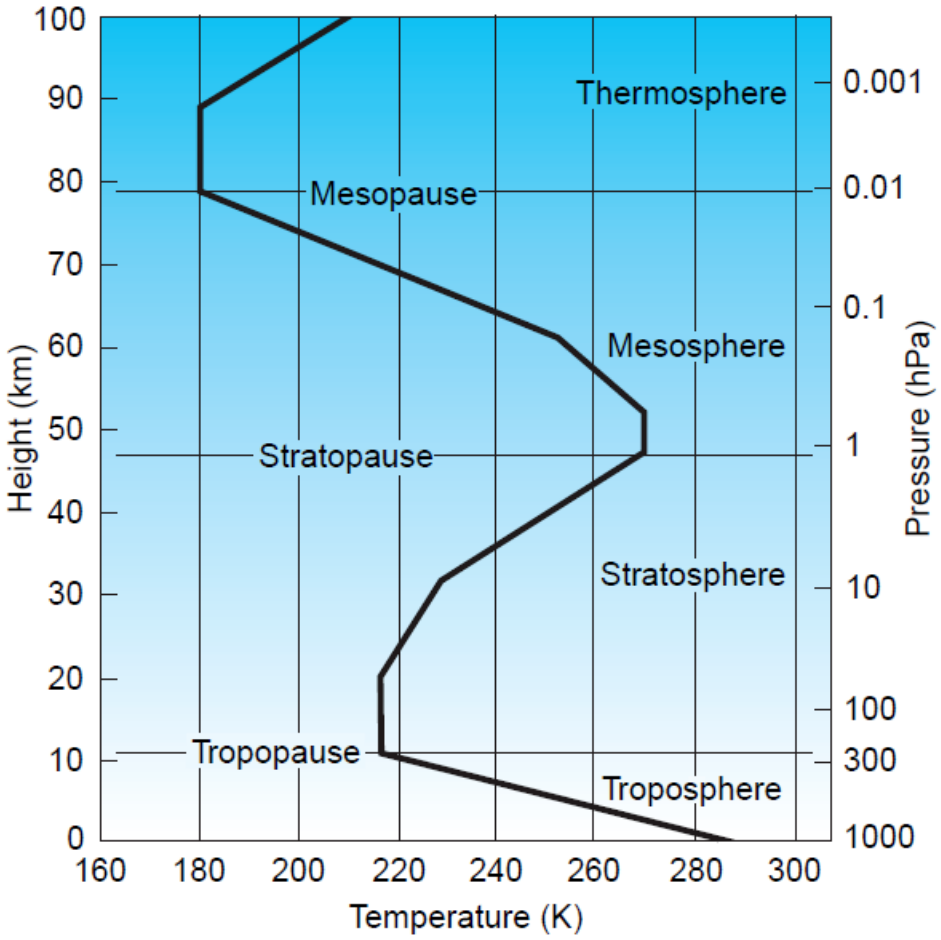

Figure 1.2 A typical midlatitude vertical temperature profile. From Wallace and Hobbs, 2006.

Stratosphere starts from tropopause to approximate height of 50 km. The stratosphere is characterized by weak vertical motions (as opposed to what happens in the troposphere) and by extremely dry and ozone rich air. The increase in temperature in this layer is caused by absorption of ultraviolet radiation by ozone (O_3). Ozone is abundant in this layer, and about 90 percent of the total ozone present in the atmosphere is concentrated in this layer. The upper limit is stratopause which is a very narrow strip of transition zone beyond which mesosphere is found. In the mesosphere temperature decreases again with height to a minimum defined mesopause. In the thermosphere, however, there is another increase in temperature with height due absorption of solar radiation, which strips electrons from atoms (photoionization) and splits diatomic nitrogen and oxygen molecules into single atoms (photodissociation).

1.2 Coordinate system in atmospheric science

Every point on the Earth's surface is adequately represented in terms of a spherical coordinate system rotating with the Earth (Figure 1.3). The coordinates are the latitude ϕ, the longitude λ and the height z above sea level. Latitude ϕ is defined as the angular distance of a point from the equator, measured in degrees (from 0° to 90°) towards the North (N) or South (S). Longitude is defined as the angular distance of a point from the Greenwich prime meridian, measured in degrees (from 0° to 180°) east (E) or west (W).

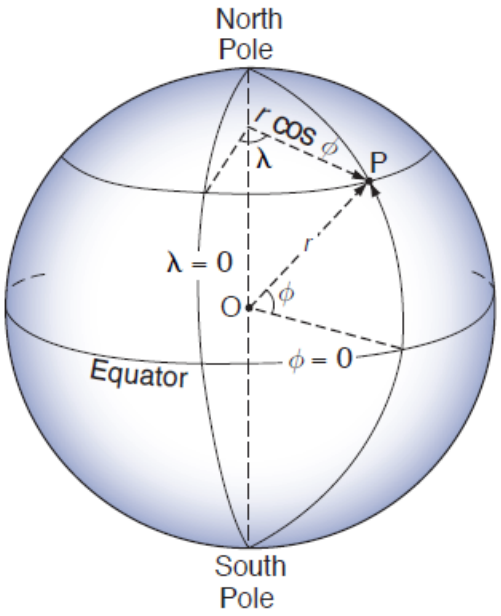

Figure 1.3- Spherical Coordinate system.
From Wallace and Hobbs 2006.

If we denote by x the distance east of the Greenwich meridian along the latitude, by y the distance north of the equator along a meridian, and by r the distance from the centre of the Earth , we will have:

$$dx = r\, d\lambda\, \cos\phi \qquad (1.3a)$$

and

$$dy = r\, d\phi. \qquad (1.3b)$$

Considering that 99.99% of the mass of the atmosphere is concentrated within 50 km of the surface, the radius r is approximated by the value of the Earth's radius R_E $(6.37x10^6\ m)$.

Consequently, motion in the atmosphere is described by the following three components of velocity:

$$u = \frac{dx}{dt} = R_E\, \cos\phi\, \frac{d\lambda}{dt} \quad (the\ zonal\ velocity\ component), \qquad (1.4a)$$

$$v = \frac{dy}{dt} = R_E\, \frac{d\phi}{dt} \quad (the\ meridional\ velocity\ component), \qquad (1.4b)$$

and

$$w = \frac{dz}{dt} = \frac{dr}{dt} \quad (the\ vertical\ velocity\ component). \qquad (1.4c)$$

The horizontal velocity **V** is defined as $\vec{\mathbf{V}} = u\hat{\mathbf{i}} + v\hat{\mathbf{j}}$ where **i** and **j** are the unit vector in the zonal and meridional direction, respectively. It is conventionally established that the zonal speed is considered positive if the wind is blowing eastward and negative if blowing westward. Similarly, the southern component is defined as positive or negative when referring to a wind blowing north or south. This is true in both the northern and southern hemispheres. Considering the scales of motion in the Earth's atmosphere, it can be said that the typical amplitude of the horizontal component V of velocity

exceeds the vertical component by several orders of magnitude. For these scales the term wind coincides with the horizontal component of velocity.

If we consider surfaces where a certain quantity, such as pressure, is constant, it is possible to construct a set of lines, called streamlines, arbitrarily spaced whose orientation is parallel everywhere at the horizontal velocity **V.** A natural coordinate system (s, n) (Figure 1.4) can be defined at each point on this surface. Where the s coordinate is directed along the line, while the n coordinate is perpendicular to it.

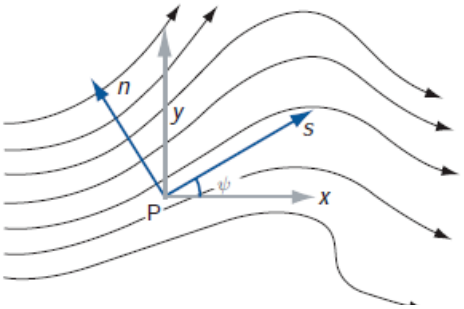

Figure1.4-Natural Coordinates (s, n) at a point P. From Wallace and Hobbs, 2006.

As regards the scalar wind speed, we can then write:

$$V = \frac{ds}{dt}\ , and\ \frac{dn}{dt} = 0.$$

As shown in Figure 1.4, the flow information is completed by angle ψ, which indicates the direction.

1.3 Atmospheric Thermodynamics

Thermodynamics plays an important role in our quantitative understanding of the atmospheric phenomena ranging for the smallest cloud microphysical processes the general circulation of the atmosphere. The purpose of the following sections is to introduce some fundamental concepts that we will encounter later in this thesis. With particular attention to the definition of two quantities: the geopotential height Z and Integrated Vapor Trasport (IVT), which we use to quantify moisture transport.

1.3.1 The postulates of thermodynamics

A thermodynamic system is a part of the universe considered to be distinct from the external environment. Thermodynamic systems, if external conditions do not change, tend to assume a state of equilibrium that we postulate to have the following properties:

- the characteristics of equilibrium states are independent of the preparation of the system, i.e. of its history,
- states of equilibrium are defined completely by knowledge of a finite number of *extensive* independent variables.

To define an extensive variable, we consider two separate thermodynamic systems, C1 and C2, each in a state of equilibrium and characterised by s variables $x_1, \dots, x_s$. Let us now consider the C system consisting of the sum (understood conceptually) of the two systems C1 and C2. The variable x_i is said to be extensive when the value it assumes in the C system is given by the sum of the values it assumes in the two systems C1 and C2.

Suppose that for any thermodynamic system there exists a physical observable A whose integral $\int A$ does not depend on the path of integration, but only on the limits of integration. We will then say that A is a thermodynamic state function. This is equivalent to saying that dA is an exact differential.

Given a differential of the form $df = f_1(A,B)dA + f_2(A,B)dB$, the condition that df is exact is $\partial f_1/\partial B = \partial f_2/\partial A$.

In an arbitrary thermodynamic transformation, let ΔQ be the net amount of heat absorbed and ΔW the work done by the system. The first law of thermodynamics states that the quantity ΔU, defined by

$$\Delta U = \Delta Q - \Delta W \tag{1.5}$$

is the same for all transformations that go from a given initial state to a given final state. This automatically defines a state function U, called internal energy. Empirically, it can be observed that U is an extensive quantity.

In an infinitesimal transformation, the first law reduces to the statement that the differential

$$dU = dQ - dW \tag{1.6}$$

is exact. Obviously, this property is not shared by dQ and dW.

The second law of thermodynamics states the existence of an extensive variable S called entropy, which is also a state function and defined only in the equilibrium states of a system.

Entropy has the following properties:

- It is always greater than or equal to zero,
- In any thermodynamic system, entropy assumes its maximum value with respect to all infinitesimal virtual variations, compatible with internal constraints, of the other extensive quantities that characterise the system,
- In an infinitesimal transformation in which the system absorbs a quantity of heat δQ at temperature T, entropy increases by a quantity equal to $\delta Q/T$ if the process is reversible and by a quantity greater than $\delta Q/T$ if the process is irreversible.

Given a function $f(x_1,..,x_s)$, this is defined as homogeneous of degree n if, for any number $\alpha \in \mathbb{R}$:

$$f(\alpha\, x_1, \dots, \alpha\, x_s) = \alpha^n\, f(x_1, \dots, x_s)\,. \tag{1.7}$$

An important property of homogeneous functions is that if $f = f(x_1,..,x_s)$, is homogeneous of degree n, its partial derivatives are homogeneous functions of degree n-1. In formulas:

$$\frac{\partial f(\alpha x_1,..,\alpha x_s)}{\partial x_k} = \sum_i \frac{\partial f(\alpha x_1,..,\alpha x_s)}{\partial(\alpha x_i)}\frac{\partial(\alpha x_i)}{\partial x_k} = \alpha\, f_k'(\alpha x_1,..,\alpha x_s)$$

$$\alpha^n \frac{\partial f(x_1,..,x_s)}{\partial x_k} = \alpha^n \sum_i \frac{\partial f(x_1,..,x_s)}{\partial(\alpha x_i)}\frac{\partial(\alpha x_i)}{\partial x_k} = \alpha^n\, f_k'(x_1,..,x_s)$$

Therefore:

$$f_k'(\alpha x_1,..,\alpha x_s) = \alpha^{n-1}\, f_k'(x_1,..,x_s)$$

Given a homogeneous function of degree n, setting $\alpha = 1 + \epsilon$, we will have:

$$f((1+\epsilon)\, x_1, \dots) = (1+\varepsilon)^n\, f(x_1, \dots, x_s) \tag{1.8}$$

Expanding the left-hand side of (1.8) in a Taylor series and taking the limit as ε approaches zero, we have:

$$f(x_1, \dots, x_s) + \varepsilon \sum_k x_k \frac{\partial f(x_1, \dots, x_s)}{\partial x_k} = (1 + n\varepsilon) f(x_1, \dots, x_s)$$

That is, for homogeneous functions of degree one, the following property holds:

$$\sum_k \frac{\partial f(x_1,\dots,x_s)}{\partial x_k} \, x_k \; = \; f(x_1, \dots, x_s) \tag{1.9}$$

Having introduced the extensive variables *S* and *U*, let us assume that the thermodynamic state of a system is described by a number *m* of other extensive variables. The equation linking *S*, *U* and the other extensive variables under equilibrium conditions is called the fundamental equation of thermodynamics. We will have:

$$f(U, S, \{x_i\}) = 0 \tag{1.10a}$$

or solving with respect to any of the variables such as U:

$$U = U(S, \{x_i\}) \tag{1.10b}$$

Since all variables appearing (1.10a) are extensive, if the system is scaled globally by a factor α, all variables will be scaled by the same factor α, i.e.:

$$U(\lambda \, S, \{\alpha \, x_i\}) = \alpha \, U(S, \{x_i\})$$

We therefore have that the postulates of thermodynamics lead to the conclusion that the fundamental equation of thermodynamics is a homogeneous function of degree one. Differentiating (1.10b) gives:

$$dU = \frac{\partial U}{\partial S} \, dS + \sum_k \frac{\partial U}{\partial x_k} \, dx_k \tag{1.11}$$

All derivatives appearing in (1.11) are homogeneous functions of degree zero of the system variables, i.e. they do not depend on the scale factor of the system itself. Thermodynamic quantities of this type are called intensive variables or state parameters.

Let us define: $\frac{\partial U}{\partial S} = T$; $\frac{\partial U}{\partial x_i} = p_i$

The intensive variable T is called thermodynamic temperature, while the variables p_i are called generalised pressures. If we consider a system in equilibrium in which no force field acts other than an external pressure P and which consists of a fixed number of molecules of a single species, the set of x_i is reduced to the single variable V, i.e. the volume of the system.

Recalling that $\frac{\partial U}{\partial V} = -P$ we will then have:

$$dU = TdS - PdV = dQ - dW \tag{1.12}$$

On several occasions, it is convenient to reformulate the fundamental equation (1.10b) using both intensive and extensive variables as independent variables. This leads to the definition of a series of state functions called thermodynamic potentials.

Some of these potentials are particularly important and have specific names:

- the enthalpy: $H(S,P,..) = U(S,V,..) + PV$ (1.13)
- Helmholtz free energy: $A(T,V,..) = U(S,V,..) - TS$ (1.14)
- Gibbs free energy: $G(T,P,..) = U(S,V,..) - TS + PV$ (1.15)

For a system in which (1.12) is applicable, the following is obtained:

$$dH = TdS + VdP\ ,\ dA = -SdT - PdV\ ,\ \ dG = -SdT + VdP \tag{1.16}$$

From (1.12) and (1.16) we can define the specific heat at constant volume and pressure:

$$C_v = \left(\frac{\mathrm{dQ}}{\mathrm{dT}}\right)_{\mathrm{v}} = \left(\frac{\mathrm{dU}}{\mathrm{dT}}\right)_{\mathrm{v}} \tag{1.17}$$

$$C_p = \left(\frac{\mathrm{dQ}}{\mathrm{dT}}\right)_{\mathrm{p}} = \left(\frac{\mathrm{dH}}{\mathrm{dT}}\right)_{\mathrm{p}} \tag{1.18}$$

Let us consider a homogeneous thermodynamic system (i.e., consisting of a single phase) containing a single chemical species, but not limited to a fixed number of molecules. In this case, among the extensive variables on which energy depends, we must also include the number N of molecules. For internal energy, we write:

$$dU = \left(\frac{\partial U}{\partial S}\right)_{V,N} dS + \left(\frac{\partial U}{\partial V}\right)_{S,N} dV + \left(\frac{\partial U}{\partial N}\right)_{V,S} dN = TdS - PdV + \mu dN$$

The third derivative μ is called the chemical potential. If we assume that the system contains m different chemical species and that N_i indicates the number of molecules of the chemical species indicated by i, we will have:

$$dU = \left(\frac{\partial U}{\partial S}\right)_{V,N_1,..,N_m} dS + \left(\frac{\partial U}{\partial V}\right)_{S,N_1,..N_m} dV + \sum_i^m \left(\frac{\partial U}{\partial N_i}\right)_{V,S,N_j} dN_i = TdS - PdV + \sum_i^m \mu_i dN_i$$

Applying the (1.9) relation:

$$U = TS - PV + \sum_i^m \mu_i N_i$$

Using the relations (1.13) -(1.15) and the differential dU, it is possible to express H, A and G even for systems with many components. For example, in the case of G, we obtain:

$$G = U + PV - TS = \sum_i^m \mu_i N_i$$

differentiating both members:

$$dG = dU + d(PV) - d(TS) = VdP - SdT + \sum_i^m \mu_i dN_i$$

$$dG = d(\sum_i^m \mu_i N_i) = \sum_i^m \mu_i dN_i + \sum_i^m N_i du_i$$

Comparing the two results yields an important relationship known as the Gibbs–Duhem equation:

$$SdT - VdP + \sum_i^m N_i du_i = 0$$

1.3.2 Gas Laws

An ideal gas is an important idealised thermodynamic system. Experimentally, all gases behave universally when sufficiently diluted, and the ideal gas is the idealisation of this limiting behaviour. The parameters of an ideal gas are pressure P, volume V, temperature T and the number of components N. In formula form:

$$PV = NkT \qquad \text{where} \quad k = 1.38\text{x}10^{-23}\ \text{J/K}$$

is called Boltzmann's constant. An equivalent form of the equation of state for an ideal gas is:

$$PV = nR^*T \qquad \text{where} \quad R^* = 8.315\ \text{J/K} \qquad (1.19)$$

is the universal gas constant and n stands for the number of moles. The number of moles n is given by:

$$n = \frac{N}{N_A} \qquad or \qquad n = \frac{m}{M}$$

where in the first equation, $N_A = 6.023x10^{23}$ is Avogadro's number (the number of molecules contained in one mole). In the second equation, m is the mass (in grams) of the gas and M is the molecular weight of the same substance expressed in grams per mole.

Because $\rho = m/V$ is the density of the gas and $\alpha = 1/\rho$ is its specific volume, we can rewrite (1.19) in these forms:

$$PV = mRT, \qquad P = \rho RT \quad \text{or} \quad P\alpha = RT \qquad (1.20)$$

in which the value of R depends in this case on the gas.

Dry air, therefore excluding water vapour from our reasoning for the moment, is a mixture of gases. The total pressure of a mixture of gases, which do not interact chemically, is given by the sum of the partial pressures of the various component gases (Dalton's Law).

Therefore, indicating this pressure with P_d (and with the prefix d for dry air), we write:

$$P_d = \sum_i P_i = \sum_i \frac{n_i R^* T}{V} = \sum_i \frac{m_i}{M_i}\ \frac{R^* T}{V} = \frac{\sum_i m_i}{V}\left(\sum_i \frac{m_i}{M_i} \Big/ \sum_i m_i\right) R^* T = \frac{m_d}{V}\frac{R^*}{M_d} T = \rho_d R_d T \qquad (1.21)$$

Similarly, for water vapor, where e denotes partial pressure exerted by the water vapor, we have:

$$e = \frac{m_v}{V}\ \frac{R^*}{M_w} T = \rho_v R_v T \qquad (1.22)$$

From (1.21) and (1.22)

$$R_d / R_v = M_d / M_w \equiv \varepsilon = 0.622 \qquad (1.23)$$

However, rather than using a gas constant for humid air, whose exact value depends on the amount of water vapour in the air, it is more convenient to use the constant for humid air and a fictitious temperature, called the virtual temperature T_v.

Considering a volume V of humid air at temperature T, its pressure P and density ρ , based on what has been said so far, will be given by the following sums:

$$P = P_d + e \qquad\qquad \rho = \frac{m_d + m_w}{V} = \rho_d + \rho_W$$

Expressing the partial densities as a function of the relative pressures, we obtain:

$$\rho = \rho_d + \rho_W = \frac{P_d}{R_d T} + \frac{e}{R_W T} = \frac{P - e}{R_d T} + \frac{e}{R_W T} = \frac{P}{R_d T}\left[1 - \frac{e}{P}(1 - \varepsilon)\right]$$

Explaining P:

$$P = \rho R_d \frac{T}{\left[1 - \frac{e}{P}(1-\varepsilon)\right]} = \rho R_d T_v \tag{1.24}$$

where we defined the virtual temperature $T_v = \frac{T}{\left[1 - \frac{e}{P}(1-\varepsilon)\right]}$. (1.25)

1.3.3 Geopotential height and Hypsometric Equation

In fluid mechanics, hydrostatic equilibrium, also called hydrostatic balance, is the condition of a fluid , which occurs when the resultant of external forces, such as gravity, are balanced by a pressure-gradient force.

To derive an important equation for the hydrostatic balance of the atmosphere, let us consider a vertical column of air with a unit cross-section, between heights z and $z + \delta z$. The mass of this column of air will then be given by $\rho(z)\delta z$, where $\rho(z)$ is the density of air at height z.

Gravity acts on this layer δz with a downward force given by $g\rho\delta z$, where g is the acceleration due to gravity. Denoting the pressure at height z by $p(z)$, we will have a pressure change $\delta p = p(z + \delta z) - p(z)$ between the two heights. Pressure decreases as height increases, therefore δp will have a negative sign in the equilibrium equation.

Therefore, hydrostatic balance requires:

$$-\delta p = g\rho\delta z$$

or, in the limit as $\delta z \to 0$,

$$\frac{\partial p}{\partial z} = -g\rho \tag{1.26}$$

Equation (1.26) is the hydrostatic equation.

Let Φ be the gravitational potential, or geopotential. The units of geopotential are J kg^{-1}. The work required to lift 1 kg from a height z to a height $z + \delta z$ will therefore be $d\Phi = gdz$. If, by convention, we assume $\Phi(0) = 0$ at sea level ($z = 0$), the geopotential $\Phi(z)$ at height z is given by:

$$\Phi(z) = \int_0^z g dz$$

We can also define a quantity called the geopotential height Z as

$$\mathrm{Z} = \frac{\Phi(z)}{g_0} = \frac{1}{g_0}\int_0^z g\,dz \tag{1.27}$$

where g_0 is the globally averaged acceleration due to gravity at Earth's surface (taken as 9.81 ms^{-2}). Geopotential height is used as the vertical coordinate in most atmospheric application in which energy plays an important role.

In meteorological practice it is not convenient to deal with the density of a gas, ρ, the value of which is generally not measured. Using (1.24) in (1.26), we obtain

$$\frac{\partial p}{\partial z} = -g\rho = -\frac{pg}{R_d T_v} \quad \Rightarrow \quad -R_d T_v \frac{dp}{p} = g\,dz = d\Phi\ .$$

If we now integrate between pressure level p_1 and p_2, with geopotential Φ_1 and Φ_2, respectively,

$$\int_{\Phi_1}^{\Phi_2} d\Phi = -\int_{p_1}^{p_2} R_d T_v \frac{dp}{p} \qquad \text{or} \qquad \Phi_2 - \Phi_1 = R_d \int_{p_2}^{p_1} T_v \frac{dp}{p}$$

Dividing both sides of the last equation by g_0

$$\mathrm{Z}_2 - \mathrm{Z}_1 = \frac{R_d}{g_0}\int_{p_2}^{p_1} T_v \frac{dp}{p} \tag{1.28}$$

For an isothermal atmosphere, if the virtual temperature correction is neglected ($T = T_v$), we can obtain an estimate for the value of H, the scale height, discussed in (1.1). Let us write:

$$\mathrm{Z}_2 - \mathrm{Z}_1 = \frac{R_d}{g_0} T \int_{p_2}^{p_1} \frac{dp}{p} = \mathrm{H} \ln\left(\frac{p_1}{p_2}\right) \qquad or \qquad p_2 = p_1 e^{-\frac{(Z_2 - Z_1)}{H}} \tag{1.29}$$

where $H = {R_d T}/{g_0} = 29.3\mathrm{T}$. For T=255K (the approximate mean value for the troposphere and stratosphere), the scale height H appears to be about 7.5 km.

The temperature of the atmosphere generally varies with height, and the virtual temperature correction cannot always be neglected. In line with what we have done so far, we will deal with this more general case in the following way.

$$\mathrm{Z}_2 - \mathrm{Z}_1 = \frac{R_d}{g_0}\int_{p_2}^{p_1} T_v \frac{dp}{p} = \frac{R_d}{g_0}\frac{\int_{p_2}^{p_1} T_v \frac{dp}{p}}{\int_{p_2}^{p_1} \frac{dp}{p}} \int_{p_2}^{p_1} \frac{dp}{p} = \frac{R_d \bar{T}_v}{g_0}\int_{p_2}^{p_1} \frac{dp}{p} = \bar{H}\int_{p_2}^{p_1} \frac{dp}{p} \tag{1.30}$$

Equation (1.30) is called the hypsometric equation.

We can therefore define geopotential height as the altitude at which a given atmospheric pressure (e.g. 850 hPa) is found at a given instant of time, calculated on the basis of the gravitational potential energy of the air column; it is fundamental in meteorology because it indicates the presence of warm air (high geopotential, "lighter" and higher air) or cold air (low geopotential, denser and "lower" air) at high altitudes, influencing atmospheric dynamics.

Let us now consider a layer of air in hydrostatic equilibrium, calculate the differential of its enthalpy (1.16) by imposing the condition of hydrostatic equilibrium (1.26):

$$dH = dQ + V dP = dQ + V\frac{dP}{dz}dz = dQ - V\rho g dz = dQ - m d\Phi$$

First, we divide by m to obtain the expressions per unit of mass, then we rearrange the equation to obtain an expression for the heat dq exchanged.

$$dq = dh + d\Phi = d(h + \Phi) = d\left(c_{\mathrm{p}}T + \Phi\right) \tag{1.31}$$

where c_{p} is the specific heat at constat pressure.

If the layer of air in question undergoes only adiabatic transformations and if its macroscopic kinetic energy is negligible compared to its total energy, we can derive an expression for the rate of change of temperature with height of a parcel of dry air:

$$0 = dq = d\left(c_{\mathrm{p}}T + \Phi\right) = c_{\mathrm{p}}dT + d\Phi = c_{\mathrm{p}}dT + gdz \Longrightarrow -\left(\frac{dT}{dz}\right)_{dry\ parcel} = \frac{g}{c_{\mathrm{p}}} \equiv \Gamma_d$$

Γ_d is called the dry adiabatic lapse rate. Substituting $g = 9.81\ \mathrm{ms}^{-2}$ and $c_{\mathrm{p}} = 1004\ \mathrm{JK}^{-1}\mathrm{kg}^{-1}$ we have $\Gamma_d = 9.8\ K\ \mathrm{km}^{-1}$.

1.3.4 Water Vapor in Air

Previously, we indicated the presence of water vapour in the air through pressure and the effect it exerts, and we quantified its effect on air density by introducing the concept of virtual temperature. However, various quantities can be considered to characterise the state of humid air, and we will introduce some of them here.

The mixing ratio *w* is defined as the ratio between the mass m_v of water vapour and the mass of dry air m_d contained in the same volume of humid air. That is

$$w \equiv \frac{m_v}{m_d} \tag{1.32}$$

since water vapour and dry air obey the ideal gas equation, and given that for the temperature ranges observed in the Earth's atmosphere, $p \gg e$, we write

$$w = \frac{\rho_v}{\rho_d} = \frac{e/R_vT}{p_d/R_dT} = \frac{R_d}{R_v}\frac{e}{p_d} = \varepsilon\frac{e}{p-e} \cong \varepsilon\frac{e}{p}$$

For convenience, the mixing ratio is usually expressed in grams of water vapor per kilogram of dry air. If neither condensation nor evaporation takes place, the mixing ratio of an air parcel is constant.

The mass of water vapor m_v in a unit of mass of air $m = m_v + m_d$ is called the specific humidity q, that is

$$q \equiv \frac{m_v}{m_v+m_d} = \frac{w}{1+w} \tag{1.33}$$

Because the magnitude of *w* is only a few percent, it follows that the numerical values of *w* and *q* are nearly equivalent.

The saturation pressure of water e_s (or saturated vapour pressure) is the pressure at which liquid water and water vapour are in dynamic equilibrium, i.e. when the rate of evaporation is equal to that of condensation, and this pressure depends heavily on temperature: as the temperature increases, the saturation pressure increases, determining the boiling point when the saturation pressure equals the external atmospheric pressure.

The saturation mixing ratio w_s is the maximum mass of water vapor m_{vs} that a specific mass of dry air m_d can hold at a given temperature and pressure before condensation occurs.

$$w_S \equiv \frac{m_{vs}}{m_d}$$

For the same arguments used for (1.32),

$$w_s = \frac{\rho_{vs}}{\rho_d} = \frac{e_s/R_v T}{p_d/R_d T} = \frac{R_d}{R_v}\frac{e_s}{p_d} = \varepsilon\frac{e_s}{p - e_s} \cong \varepsilon\frac{e_s}{p}$$

The relativity humidity (RH) is the ratio (expressed as percentage) between the mixing ratio w and the saturation mixing ratio w_s at the same temperature and total pressure. That is

$$RH = 100\frac{w}{w_s} \cong 100\frac{e}{e_s}$$

1.3.5 Clausius-Clapeyron equation

Let us now consider a system in equilibrium consisting of a single component present in two phases, which we denote as α and β. Since the system is in equilibrium, all generalised pressures have the same value in both phases.

For the generic extensive quantity Y, we can write: $Y = Y_\alpha + Y_\beta = n_\alpha y_\alpha + n_\beta y_\beta$, where n_α and n_β are the number of moles of the two phases, while y_α and y_β, called the molar quantities of the pure component of phases α and β, are obtained by deriving Y_α and Y_β with respect to $n_\alpha$and n_β and represent respectively the value of Y for one gram molecule of each phase. y_α and y_β are intensive quantities, functions of T and P.

Applying this to Gibbs free energy, we get:

$$G = G_\alpha + G_\beta = n_\alpha\mu_\alpha + \mu_\beta y_\beta \quad \text{where} \quad \mu_\alpha = \frac{\partial G_\beta}{\partial n_\alpha},\ \mu_\beta = \frac{\partial G_\beta}{\partial n_\beta}$$

So, for phase α, it will be:

$$d\mu_\alpha = \left(\frac{\partial\mu_\alpha}{\partial P}\right)_T dP + \left(\frac{\partial\mu_\alpha}{\partial T}\right)_P dT = \left(\frac{\partial^2 G_\alpha}{\partial P\partial n_\alpha}\right)dP + \left(\frac{\partial^2 G_\alpha}{\partial T\partial n_\alpha}\right)dT$$

$$= \left(\frac{\partial V_\alpha}{\partial n_\alpha}\right)_T dP + \left(\frac{\partial(-S_\alpha)_\alpha}{\partial n_\alpha}\right)_T dT = \nu_\alpha dP - s_\alpha dT$$

With a similar relationship for phase β. Because at equilibrium $\mu_\alpha = \mu_\beta$, throughout the entire range of coexistence of the two phases, the following relationship will apply: $d\mu_\alpha = d\mu_\beta$. That is,

$$\nu_\alpha dP - s_\alpha dT = \nu_\beta dP - s_\beta dT \implies \frac{dP}{dT} = \frac{s_\alpha - s_\beta}{\nu_\alpha - \nu_\beta} = \frac{l}{T\Delta\nu} \tag{1.34}$$

Where (1.34), known as the Clausius-Clapeyron equation, establishes the condition of equilibrium between two phases of the same component as temperature and pressure vary. The quantity $l = T\Delta s$ is called the latent heat of transition. Latent heat of transition is the amount of thermal energy that a substance absorbs or releases when it changes from one state of aggregation to another without its temperature changing.

1.4 Atmospheric Dynamics

Atmospheric dynamics studies the movements of air masses and the physical processes that regulate weather and climate on different spatial and temporal scales. This section aims to illustrate the salient aspects of large-scale dynamics on a rotating planet, to introduce the system of primitive equations widely used to predict how these motions evolve over time.

1.4.1 Forces influencing atmospheric motion

Large-scale motions involve horizontal scales of thousands of kilometres or more, vertical scales of the order of the height of the tropopause, and time scales of a day or more. Motions on these scales occur in hydrostatic equilibrium (1.26), are directly influenced by the Earth's rotation, and have a vertical component of their three-dimensional velocity vector that is much smaller than the horizontal component. Therefore, in the following pages, we propose to derive the horizontal components of the forces that govern atmospheric motions**.**

Atmospheric motion is mainly influenced by three forces: the Pressure Gradient Force (which moves air from high to low pressure), the Coriolis Force (due to the Earth's rotation, which deflects winds to the right in the northern hemisphere and to the left in the southern hemisphere), and Friction (which slows down the movement of air near the surface). These forces interact to create winds and influence the formation of pressure systems and storms.

Motion in a rotating coordinate system (Appendix A) occurs as if three complementary inertial forces act on each moving point **R**(t) of mass m: centrifugal force $m\boldsymbol{\Omega}x(\boldsymbol{\Omega}\mathrm{x}\mathbf{R})$, Coriolis force $2m\boldsymbol{\Omega}x\dot{\boldsymbol{R}}$, and rotational inertial force $\mathrm{m}\dot{\boldsymbol{\Omega}}x\boldsymbol{R}$ ($\boldsymbol{\Omega}$ is the angular velocity vector). And so:

$$m\ddot{\boldsymbol{R}} = \boldsymbol{F}\left(\boldsymbol{R},\dot{\boldsymbol{R}}\right) - 2m\boldsymbol{\Omega}x\dot{\boldsymbol{R}} - m\boldsymbol{\Omega}x(\boldsymbol{\Omega}\mathrm{x}\mathbf{R}) - \mathrm{m}\dot{\boldsymbol{\Omega}}x\boldsymbol{R}$$

The third of these three inertial forces is only observed in the case of non-uniform rotation; the first and the second also exist for uniform rotations. Centrifugal force always acts in the direction away from the instantaneous axis of rotation. This force does not depend on the speed of relative motion and acts on bodies at rest. Coriolis force depends on speed.

Since the rotation of the Earth can be considered uniform ($\dot{\boldsymbol{\Omega}} = 0$), and $\boldsymbol{F}\left(\boldsymbol{R},\dot{\boldsymbol{R}}\right) = mg^*$ (where g^* is the acceleration due to gravity), we can write (including centrifugal acceleration in g):

$$m\ddot{\boldsymbol{R}} = m\left(\boldsymbol{g}^* - \boldsymbol{\Omega}x(\boldsymbol{\Omega}\mathrm{x}\mathbf{R})\right) - 2m\boldsymbol{\Omega}x\dot{\boldsymbol{R}} = m\boldsymbol{g} - 2m\boldsymbol{\Omega}x\dot{\boldsymbol{R}}$$

The horizontal component of the Coriolis term is often written in the form:

$$\boldsymbol{C} = -f\boldsymbol{k}x\boldsymbol{V} = fv\boldsymbol{i} - fu\boldsymbol{j} \qquad (1.35)$$

where $f = 2\Omega\sin\phi$ is called Coriolis parameter and **k** is the local vertical unit vector, defined as positive upward.

In an elementary volume of gas with dimensions dx, dy, and dz, if we consider the pressure forces on two opposite faces, we have for the face at x_0 an inward force equal to $F_0 = p(x_0)dy\,dz$. On the opposite face (at $x_1 = x_0 + \delta x$) we have a force $F_1 = -p(x_0 + dx)dy\,dz$. With a Taylor series expansion, we have:

$$p(x_0 + \delta x) = p(x_0) + \left(\frac{\partial p}{\partial x}\right)_{x_0} dx$$

From which the component of force along x-direction is found to be:

$$F_{\mathrm{x}} = F_1 + F_0 = \left(\frac{\partial p}{\partial x}\right)_{x_0} dx\,dy\,dz$$

A similar result is obtained for the y-direction and for the z-direction. Dividing by $\rho dxdydz$ gives the force per unit mass, called the pressure gradient force.

$$\boldsymbol{P} = -\frac{1}{\rho}\frac{\partial p}{\partial x}\,\boldsymbol{i} - \frac{1}{\rho}\frac{\partial p}{\partial y}\boldsymbol{j} - \frac{1}{\rho}\frac{\partial p}{\partial z}\,\boldsymbol{k} = -\frac{1}{\rho}\nabla p \tag{1.34}$$

For the horizontal component only:

$$\boldsymbol{P}_{\mathbf{h}} = -\frac{1}{\rho}\frac{\partial p}{\partial x}\,\boldsymbol{i} - \frac{1}{\rho}\frac{\partial p}{\partial y}\boldsymbol{j} = -\frac{1}{\rho}\nabla_z p \tag{1.35}$$

If, instead of using the coordinates (x, y, z), we wanted to use the coordinates (x, y, p), let us begin by defining a function φ in the two different coordinate systems.

$$\varphi_{\mathrm{z}}(\mathrm{x},\mathrm{y},\mathrm{z}) = \varphi_{\mathrm{p}}(\mathrm{x},\mathrm{y},\mathrm{p}(\mathrm{x},\mathrm{y},\mathrm{z}))\ \text{ we write}$$

$$\left(\frac{\partial\varphi_{\mathrm{z}}}{\partial \mathrm{x}}\right)_{\mathrm{y,z}} = \left(\frac{\partial\varphi_{\mathrm{p}}}{\partial \mathrm{x}}\right)_{\mathrm{y,p}} + \frac{\partial\varphi_{\mathrm{p}}}{\partial \mathrm{p}}\left(\frac{\partial \mathrm{p}}{\partial \mathrm{x}}\right)_{\mathrm{y,z}} \quad \text{and} \quad \left(\frac{\partial\varphi_{\mathrm{z}}}{\partial \mathrm{y}}\right)_{\mathrm{x,z}} = \left(\frac{\partial\varphi_{\mathrm{p}}}{\partial \mathrm{y}}\right)_{\mathrm{x,p}} + \frac{\partial\varphi_{\mathrm{p}}}{\partial \mathrm{p}}\left(\frac{\partial \mathrm{p}}{\partial \mathrm{y}}\right)_{\mathrm{x,z}}$$

$$\nabla_{\mathrm{z}}\varphi_z = \left(\frac{\partial\varphi_{\mathrm{z}}}{\partial \mathrm{x}}\right)_{\mathrm{y,z}}\boldsymbol{i} + \left(\frac{\partial\varphi_{\mathrm{z}}}{\partial \mathrm{y}}\right)_{\mathrm{x,z}}\boldsymbol{j} = \nabla_p\varphi_p + \frac{\partial\varphi_p}{\partial p}\nabla_z p\ .$$

If we assume $\varphi_z = \varphi_p = z$: $\nabla_z z = \nabla_p z + \frac{\partial z}{\partial p}\nabla_z p$, but $\nabla_z z = 0$, so $\nabla_p z = -\frac{\partial z}{\partial p}\nabla_z p$.

Let us recall the hydrostatic equation (1.26):

$$\nabla_{\mathrm{p}} z = -\frac{\partial z}{\partial p}\nabla_{\mathrm{z}} p = \frac{1}{g\rho}\nabla_{\mathrm{z}} p \quad \text{by which we can write}$$

$$\boldsymbol{P}_{\mathbf{h}} = -\frac{1}{\rho}\nabla_{\mathrm{z}} p = -g\nabla_{\mathrm{p}} z = -\nabla_p \Phi = -g_0\nabla_{\mathrm{p}}\mathrm{Z} \tag{1.36}$$

The frictional force (per unit mass) is given by

$$\boldsymbol{F}_{\mathbf{f}} = -\frac{1}{\rho}\frac{\partial \tau}{\partial z} \tag{1.37}$$

where τ represents the vertical component of the shear stress (i.e., the rate of vertical exchange of horizontal momentum). Frictional forces are negligible in most of the atmosphere, but not in the planetary boundary layer.

From what we have seen so far, we can say that the horizontal component of the force per unit mass acting in the atmosphere is:

$$\frac{d\boldsymbol{V}}{dt} = \boldsymbol{P} + \boldsymbol{C} + \boldsymbol{F_f} = -\frac{1}{\rho}\nabla_z p - f\boldsymbol{k}x\boldsymbol{V} + \boldsymbol{F_f} = -\nabla_p \Phi - f\boldsymbol{k}x\boldsymbol{V} + \boldsymbol{F_f} \qquad (1.38)$$

In the free atmosphere, where we can neglect the effect of friction forces, the horizontal balance of the Coriolis force and the pressure gradient allows us to define the geostrophic wind $\boldsymbol{V_g}$. In this wind, air masses move parallel to isobars (lines consisting of points of equal pressure), leaving low pressure to the left. Therefore, the approximation represented by the geostrophic wind can represent a real wind when the friction force is very small, for example over oceans or at high latitudes.

In formula:

Balance $-\nabla_p \Phi \cong f\boldsymbol{k}x\boldsymbol{V}$ applying $\boldsymbol{k}$ to both sides $-\boldsymbol{k}x\nabla_p \Phi \cong f\boldsymbol{k}x(\boldsymbol{k}x\boldsymbol{V}) = -f\boldsymbol{V}$ we have

$$\boldsymbol{V} \cong \frac{1}{f}\boldsymbol{k}x\nabla_p \Phi = \frac{g_0}{f}\boldsymbol{k}x\nabla_p Z = \frac{1}{\rho f}\boldsymbol{k}x\nabla_z p \equiv \boldsymbol{V_g} \qquad (1.39)$$

In either hemisphere, the geostrophic wind field circulates cyclonically around a centre of low pressure. Where cyclonic circulation denotes a counterclockwise circulation in the northern hemisphere and a clockwise circulation in the southern hemisphere. Instead, anticyclonic circulation refers to the movement of air around an area of high pressure (anticyclone), with winds rotating clockwise in the northern hemisphere, creating fair weather conditions.

Considering the hypsometric equation (1.30) and subtracting the two geostrophic wind equations at levels $p1$ and $p2$:

$$\Delta\boldsymbol{V_g} = \boldsymbol{V_g}(p_2) - \boldsymbol{V_g}(p_1) = \frac{g_0}{f}\boldsymbol{k}x\nabla_p\big(Z(p_2) - Z(p_1)\big) = \frac{R_d}{f}\ln\left(\frac{p_1}{p_2}\right)(\boldsymbol{k}x\nabla_p \bar{T}_v) \qquad (1.40)$$

This expression is known as thermal wind equation. Like the geostrophic wind is proportional to the gradient of height geopotential on a surface at constant pressure, the thermal wind is proportional to the gradient of thickness between two baric surfaces, i.e. to the temperature gradient.

The thermal wind is not zero if the temperature field varies horizontally differently from the pressure. Two possible configurations:

- Barotropic atmosphere $\nabla T = 0$: The isothermal surfaces coincide with the isobaric surfaces. The geostrophic wind does not vary with height, as there are no temperature differences that generate the 'thermal wind'.
- Baroclinic atmosphere: The temperature varies along the isobaric surfaces. The geostrophic wind changes intensity and direction with increasing altitude.

1.4.2 The Thermodynamic Energy Equation

From the first law of thermodynamics:

$$dq = J\,dt = c_p dT - \alpha dp$$

where J (J $\mathrm{kg}^{-1}\mathrm{s}^{-1}$) is the heating rate and represents the heat input per unit time and unit mass. Dividing by dt and rearranging the order of the terms:

$$c_p \frac{dT}{dt} - \alpha \frac{dp}{dt} + J$$

Since $\alpha = {RT}/{p}$, $\kappa = {R}/{c_p}$ and $\omega = {dp}/{dt}$, we obtain the thermodynamic energy equation:

$$\frac{dT}{dt} = \frac{\kappa T}{p}\omega + \frac{J}{c_p} \tag{1.41}$$

which determines the temperature variation along the trajectory due to the rate of heating by adiabatic compression and by heat exchange with the environment.

1.4.3 The Continuity Equation

Let us consider an infinitesimal parcel of air shaped like a block with dimensions $\delta x, \delta y,$ and δz. Its mass will be:

$$\delta M = \rho\,\delta x\,\delta y\,\delta z = -\frac{\delta x\,\delta y\,\delta p}{g}$$

where in the last step we used the hydrostatic balance equation $-\delta p = g\rho\delta z$. Because the mass of the block is not changing with time,

$$0 = \frac{d}{dt}(\delta x\,\delta y\,\delta p) = \delta y\,\delta p\frac{d}{dt}\delta x + \delta x\,\delta p\frac{d}{dt}\delta y + \delta x\,\delta y\frac{d}{dt}\delta p$$

$$0 = \delta y\,\delta p\,\delta\frac{dx}{dt} + \delta x\,\delta p\,\delta\frac{dy}{dt} + \delta x\,\delta y\delta\frac{dp}{dt} = \delta y\,\delta p\,\delta u + \delta x\,\delta p\,\delta v + \delta x\,\delta y\,\delta\omega$$

$$0 = \delta y\,\delta p\,\frac{\delta u}{\partial x}\delta x + \delta x\,\delta p\,\frac{\delta v}{\delta y}\delta y + \delta x\,\delta y\,\frac{\delta\omega}{\delta p}\delta p$$

and thus, we obtain the continuity equation:

$$\frac{\partial u}{\partial x} + \frac{\partial v}{\partial y} + \frac{\partial \omega}{\partial p} = 0$$

$$\text{or} \qquad \frac{\partial \omega}{\partial p} = -\left(\frac{\partial u}{\partial x} + \frac{\partial v}{\partial y}\right) = -\nabla\cdot\mathbf{V} \tag{1.42}$$

The divergence of the horizontal wind is linked to vertical motion: horizontal divergence $\nabla\cdot\mathbf{V} > 0$ corresponds to vertical compression $\partial\omega/\partial p < 0$, while horizontal convergence $\nabla\cdot\mathbf{V} < 0$ is associated with vertical stretching $\partial\omega/\partial p > 0$.

1.4.4 Equation of vertical motion

As we have already seen, it can be useful to transform from height (x, y, z) to pressure (x, y, p) coordinates. The coordinate change is relatively simple since z and p are related through the hydrostatic equation $-\delta p = g\rho\delta z$. The vertical velocity component in (x, y, p) is $\omega = dp/dt$ and, since p decreases with height, it is positive for sinking motion and negative for rising motion. Vertical velocity in (x, y, z) is given by $w = dz/dt$ and has opposite sign with respect to ω. Through the chain rule it is possible to obtain:

$$\omega \equiv \frac{dp}{dt} = \frac{\partial p}{\partial t} + \boldsymbol{V} \cdot \nabla_z p + w\frac{\partial p}{\partial z} = -\rho g w + \frac{\partial p}{\partial t} + \boldsymbol{V} \cdot \nabla_z p \tag{1.43}$$

In the lowest part of the atmosphere, 1–2 km, w and ω are forced to be small due to the presence of the lower boundary. At the Earth's surface the vertical velocity is

$$w_{\mathrm{s}} = \boldsymbol{V} \cdot \nabla z_{\mathrm{s}} \tag{1.44}$$

where z_{s} is the height of the terrain.

In (x, y, z) coordinates the vertical component of the newtonian equation of motion is given by

$$\frac{dw}{dt} = -\frac{1}{\rho}\frac{\partial p}{\partial z} - g + C_{\mathrm{z}} + F_{\mathrm{z}} \tag{1.45}$$

where C_{z} and F_{z} are the vertical component of the Coriolis and frictional forces, respectively. For large scale motions, in which virtually all the kinetic energy resides in the horizontal wind component, the vertical acceleration is so small in comparison to the leading terms in (1.45). In view of this, the vertical equation of motion (1.45) can be replaced by the hydrostatic equation (1.26) or, in pressure coordinates, by the hypsometric equation (1.30).

1.4.5 The Primitive Equations

In summary, the system of primitive equation is composed by:

- $\frac{d\boldsymbol{V}}{dt} = -\nabla_{\mathrm{p}}\Phi - f\boldsymbol{k}x\boldsymbol{V} + \boldsymbol{F}_{\mathbf{f}}$ (the horizontal equation of motion) (1.46)
- $\frac{\partial \Phi}{\partial p} = -\frac{RT}{p}$ (the hypsometric equation) (1.47)
- $\frac{dT}{dt} = \frac{\kappa T}{p}\omega + \frac{J}{c_p}$ (the thermodynamic energy equation) (1.48)
- $\frac{\partial \omega}{\partial p} = -\left(\frac{\partial u}{\partial x} + \frac{\partial v}{\partial y}\right) = -\nabla \cdot \mathbf{V}$ (the continuity equation) (1.49)

The complexity of the system of equations describing atmospheric dynamics makes it impossible to find an analytical solution to the problem, unless significant simplifications are made.

For primitive equations, it is possible to seek approximate numerical solutions, for example by estimating the values of the quantities on a finite number of points arranged on a grid at different vertical levels.

1.5 Integral Vapor Trasport (IVT)

Horizontal moisture and transport can be characterized by the Integral Vapor Trasport (IVT). This variable is defined as a measure of the horizontal transport of specific humidity, by integrating it for a vertical column of the troposphere.

In formula:

$$\mathbf{IVT} = \frac{1}{g_0}\int_{\mathrm{psfc}}^{\mathrm{ptop}} q\mathbf{V}\, dp \tag{1.50}$$

If we explain the components:

$$\mathrm{IVTu} = \frac{1}{g_0}\int_{\mathrm{psfc}}^{\mathrm{ptop}} qu\, dp \qquad\qquad \mathrm{IVTv} = \frac{1}{g_0}\int_{\mathrm{psfc}}^{\mathrm{ptop}} qv\, dp \tag{1.51}$$

Where q is the specific humidity (1.33), u and v are the zonal and meridional velocity component of wind, **V** is the horizontal velocity of wind, dp is the pressure increment, g_0 is the acceleration due to gravity, p_{sfc} is the surface pressure and p_{top} is the upper limit of data.
The amplitude of the IVT vector is therefore:

$$\mathrm{IVT} = \left[\left(\frac{1}{g_0}\int_{p_{sfc}}^{p_{\mathrm{top}}} qu\, dp\right)^2 + \left(\frac{1}{g_0}\int_{p_{sfc}}^{p_{\mathrm{top}}} qv\, dp\right)^2\right]^{1/2} \tag{1.52}$$

Figures 1.5 and 1.6 show maps of IVT in the eastern Mediterranean at two different times on the day a medium-intensity cyclone began. The colours represent the amplitude of the IVT, the arrows represent the direction of the IVT vector at that specific moment, and the red arrow indicates the point of maximum IVT. These representations were created using data downloaded from the ERA5 dataset.

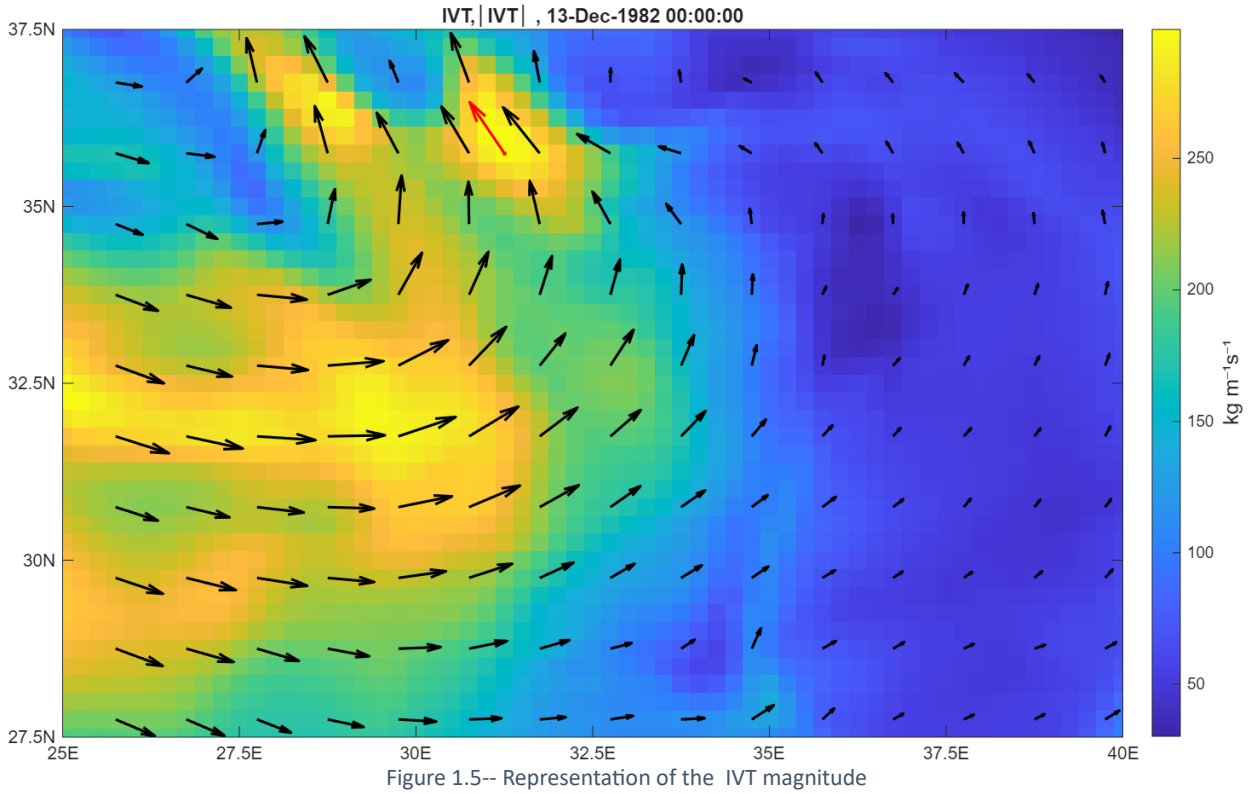

Figure 1.5-- Representation of the IVT magnitude

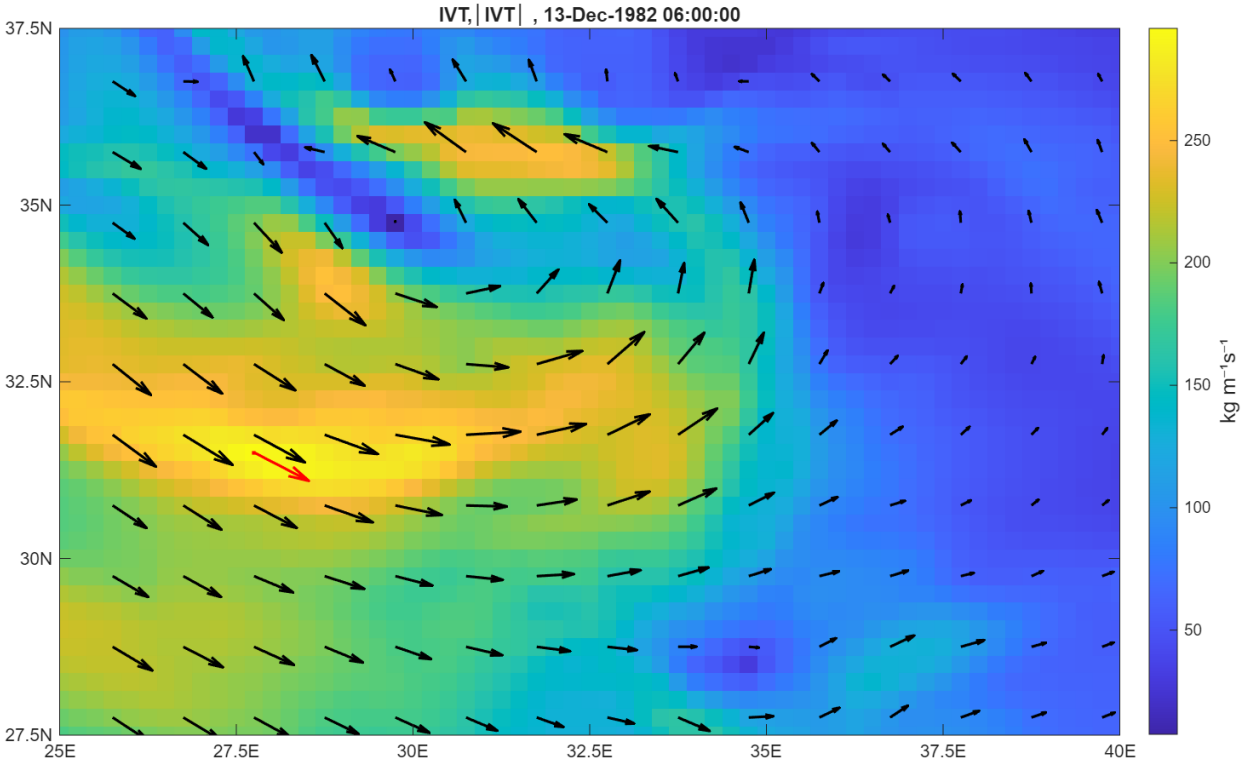

Figure 1.6- Representation of the IVT magnitude

Analysis of the formulas shows that the unit of measurement for IVT is $\mathrm{kg\,m^{-1}s^{-1}}$. The IVT has been widely used to track Atmospheric Rivers (AR). Atmospheric rivers consist of narrow bands of enhanced water vapor transport, typically along the boundaries between large areas of divergent surface air flow.

Another variable that only indicates the availability of moisture is Integrated Water Vapor (IWV). IWV is defined as the total amount of water vapor in a vertical column of the atmosphere, measured from the ground to space. Its unit of measurement is $\mathrm{kg/m^2}$.

In formula:

$$\mathrm{IWV} = \frac{1}{g_0}\int_{\mathrm{p_{sfc}}}^{\mathrm{p_{top}}} q\ dp \tag{1.53}$$

Chapter 2

Dynamical Systems

A dynamic system is a mathematical model that describes how a system evolves over time, characterised by a set of state variables that change according to precise laws, often expressed by differential equations. At the end of the first chapter, we encountered the primitive equations (Section 1.4.5), a system of nonlinear differential equations that describe the movements of fluids in the atmosphere.

Atmospheric flows are characterized by chaotic dynamics and recurring large-scale patterns. These two characteristics point to the existence of an atmospheric attractor defined by Lorentz as: "the collection of all states that system can assume or approach again and again, as opposed to those that it will ultimately avoid". The most important characteristic of chaotic motions is that it very sensitive to the change in initial conditions. That is to say that a slight change in the initial condition will completely change the final solution of the equation describing a deterministic system.

The average dimension D of the attractor corresponds to the number of degrees of freedom sufficient to describe the atmospheric circulation. Moreover, D does not provide information on transient atmospheric motions, such as those leading to weather extremes. Recent developments in dynamical systems theory show that such motions can be classified through instantaneous properties of the attractor. The instantaneous properties are uniquely determined by instantaneous dimension and stability. The concept of instantaneous dimension is intuitive: for a state Γ of the attractor (an atmospheric configuration), the instantaneous dimension $d(\Gamma)$ measures the density of neighbouring points. The stability of the state Γ is measured by $\theta(\Gamma)$ defined as the inverse of the average persistence time of trajectories around Γ. If Γ is a fixed point of the dynamics, $\theta(\Gamma) = 0$. For a trajectory that leaves the neighbourhood of Γ immediately, $\theta(\Gamma) = 1$.

This chapter introduces some basic concepts of dynamical systems, concepts that will allow us to define the local dimension d and inverse of persistence θ. Metrics used to quantify intrinsic predictability.

2.1 Basic properties

An example of a dynamic system is the system of first-order differential equations,

$$\begin{cases} \frac{dx_1}{dt} = F_1(x_1, x_2, \dots., x_n, t) \\ \frac{dx_2}{dt} = F_2(x_1, x_2, \dots., x_n, t) \\ \vdots \\ \frac{dx_n}{dt} = F_n(x_1, x_2, \dots., x_n, t) \end{cases} \tag{2.1}$$

which we shall often write in vector form as

$$\frac{d\boldsymbol{x}(t)}{dt} = \mathbf{F}[\boldsymbol{x}(t), t] \tag{2.2}$$

where **F** is a map $\mathbf{F}: Ix\Omega \ni (t, \boldsymbol{x}) \longrightarrow \mathbf{F}(t, \boldsymbol{x}) \in \mathbb{R}^n$, I is an open interval of $\mathbb{R}$ and Ω is an open interval of $\mathbb{R}^n$, defined so that **F** is continuous and locally Lipschitz function.

The system (2.1) is called linear when **F** is in the form $\boldsymbol{F}(\boldsymbol{x}(t), t) = A(t)\boldsymbol{x} + \boldsymbol{b}(t)$, where A is a matrix $A \in M(n, \mathbb{R})$ and $\boldsymbol{b}(t)$ is a continuous map $\boldsymbol{b}(t) \in C^0(I, \mathbb{R}^n)$. The system (2.1) is said to be homogeneous when $\boldsymbol{b}(t) = 0$.

Finally, the system (2.1) is defined as autonomous when f is independent of time,

$$\dot{\boldsymbol{x}} = \mathbf{F}(\boldsymbol{x}) \tag{2.3}$$

In principle for any state of the system $\boldsymbol{x}_0 = \boldsymbol{x}(0)$ we can solve the equations to obtain the future system $\boldsymbol{x}(t)$ for $t > 0$ (Cauchy problem).

A function $\boldsymbol{\phi}(t): U \subset I \longrightarrow \Omega \subset \mathbb{R}^n$ will be defined as a solution of the dynamic system (2.1) if $\dot{\boldsymbol{\phi}}(t) = \boldsymbol{F}[\boldsymbol{\phi}(t), t]$. In particular, the solutions to Cauchy's problems will be denoted as $\boldsymbol{\phi}(t; \boldsymbol{x}_0)$. Furthermore, it is common to refer to a continuous-time dynamic system as a flow.
More explicitly, the group with a single parameter of phase space transformations is called phase flow:

$$\boldsymbol{\phi}^t(\boldsymbol{x}_0): (\boldsymbol{x}_0, \mathrm{t}) \ni \Omega \mathrm{x} \mathbb{R} \longmapsto \boldsymbol{x}(t) \ni \Omega \qquad \boldsymbol{\phi}^t(\boldsymbol{x}_0) \equiv \boldsymbol{\phi}(t; \boldsymbol{x}_0). \tag{2.4}$$

with $\boldsymbol{\phi}^0(\boldsymbol{x}_0) = \boldsymbol{x}_0$ and $\boldsymbol{\phi}^s\boldsymbol{\phi}^t(\boldsymbol{x}_0) = \boldsymbol{\phi}^{t+s}(\boldsymbol{x}_0)$.
An effective and convenient tool in the study of dynamic systems is the concept of phase space. The space structured by the variables of a dynamic state system is the phase space. Thus, a one-to-one relationship is created between a state of the system and a point in the phase space. The state of the system at each moment corresponds to a point in the phase space, whereas the variation of the state with time corresponds to a curve in the phase space. The former is called a phase point, the latter a trajectory or orbit.

Let us consider an autonomous system of differential equations $\dot{\boldsymbol{x}} = \mathbf{F}(\boldsymbol{x})$ (2.3) and let $\boldsymbol{\phi}^t$ be the corresponding group of transformations,

$$\boldsymbol{\phi}^t(\boldsymbol{x}) = \boldsymbol{x} + \mathbf{F}(\boldsymbol{x})t + O(t^2) \qquad (t \longrightarrow 0) \tag{2.5}$$

Suppose S_0 be a region of phase space with volume $V(t_0)$. Then $V(t)$ will be the volume of a region S_t of phase space such that $S_t = \boldsymbol{\phi}^t S_0$. It can be shown that the following relationship is true (Appendix B):

$$\left.\frac{dV(t)}{dt}\right|_{t=t_0} = \int_{S_0} \nabla \cdot \mathbf{F} dx \qquad (dx = dx_1\, dx_2 \cdots dx_n) \tag{2.6}$$

A system in which the flow preserves volumes in phase space is called conservative. On the other hand, if the flow does not preserve volumes, and cannot be made to do so by a change of variables, then we say that the system is nonconservative.

The Lorentz-63 system was originally derived from a simplified model of atmospheric convection process and has been widely used as an example to study "chaotic" dynamical systems. Its governing can be written as:

$$\begin{cases} \dot{x} = \sigma(y - x) \\ \dot{y} = x(\varrho - z) - y \\ \dot{z} = xy - \beta z \end{cases} \tag{2.7}$$

Here σ, ρ, β >0 are parameter: σ is the Prandtl number (ratio between kinematic viscosity and thermal diffusivity), ρ is the Rayleigh number and β is a geometric parameter. x, y, z are the state variables:

x represents the convection rate, y represents the horizontal temperature variation, and z represents the vertical temperature variation.
From equations (2.7) we have that $\nabla \cdot \mathbf{F} = -(\sigma + 1 + \beta) = -v$, which is independent of the phase space position **x** and is negative. From (2.6) , we have $dV/dt = \exp(-vt)\,V(0)$. In general, $\nabla \cdot \mathbf{F}$ will be a function of phase space position **x**. If $\nabla \cdot \mathbf{F} < 0$ in some region of phase space, then we shall refer to the system as a dissipative system. It is an important concept in dynamics that dissipative systems are typically characterized by the presence of attracting sets, or attractors, in the phase space. These are bounded subsets to which regions of initial conditions of nonzero phase space volume asymptote as time increase (conservative dynamical systems do not have attractors).
The Lorentz-63 system (2.7) for some choice of the parameters (σ, ρ, β) exhibits the so-called sensitive dependence on initial condition characterizing, for which two bounded trajectory that slightly differ at some time t, will eventually be very far apart as time goes on, even though the system is deterministic and can be thus completely reconstructed given the initial condition. A trajectory is said to be bounded if there exists a ball in phase space, such that $x(t) < R < \infty$, $\forall t \in R$.

Discrete time dynamical systems are also called maps and are defined by evolution equation (with n denoting the time variable, n=0,1,2...),

$$\boldsymbol{x}_{n+1} = \boldsymbol{m}(\boldsymbol{x}_n)$$

where $\boldsymbol{m}$ is a continuous first order derivates map. If $\boldsymbol{x}_0$ is the initial state, we obtain the state at n time

$$\boldsymbol{x}_n = \boldsymbol{m}(\boldsymbol{x}_{n-1}) = \boldsymbol{m}(\boldsymbol{m}(\boldsymbol{x}_{n-2})\,) = (\boldsymbol{m} \circ \boldsymbol{m} \circ \dots\dots\dots \boldsymbol{m})(\boldsymbol{x}_0)$$

Again, we can define a discrete flow $\boldsymbol{\phi}^n(\boldsymbol{x})\colon \mathbb{N}x\Omega \longrightarrow \Omega \quad (\Omega \subset \mathbb{R}^n)$

$$\boldsymbol{\phi}^n(\boldsymbol{x}_0) \equiv \boldsymbol{x}_n : n \geq 0, \quad \boldsymbol{x}_{n+1} = \boldsymbol{m}(\boldsymbol{x}_n)$$

It is often useful to reduce a continuous time system to a discrete map by a technique called Poincaré surface of section method. The Poincaré map reduces N-dimensional flow to an (N-1)-dimensional map. The construction is done as follow: for a generic N-dimensional system, take a generic N − 1 dimensional surface in the phase space and observe the intersection of the orbit with the surface, as shown in Figure 2.1 for N = 3. Points A and B represent two consecutive points of intersection. It should be noted that B is uniquely determined by A, as it represents the evolution of the dynamics by setting A as the initial condition. Conversely, A is uniquely determined by B by reversing the flow of time. Therefore, Poincarè sections allow us to build N − 1 dimensional invertible maps.

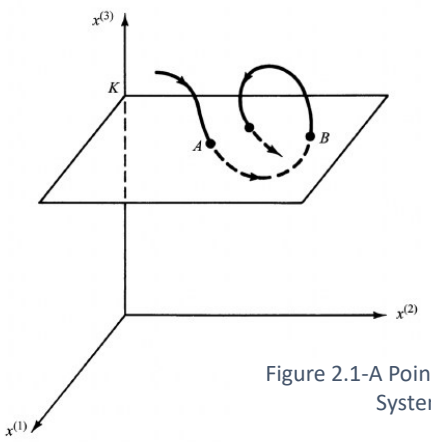

Figure 2.1-A Poincaré Surface of section. From Chaos in Dynamical Systems. Cambridge University Press, 2 editions *(2002]*

2.2 Attractors

In many cases the evolution of a dynamical system seems to converge asymptotically to a certain a set in the phase space, called attractor.

More formally, we can define an attractor to be a closed set $\mathbb{A}$ with the following properties:

1. $\mathbb{A}$ is an invariant set: any trajectory $\mathbf{x}(t)$ that starts in $\mathbb{A}$ stays in $\mathbb{A}$ for all time : $\mathbb{A} = \phi^t \mathbb{A}$.
2. $\mathbb{A}$ attracts an open set of initial conditions: there is an open set U containing $\mathbb{A}$ such that if $\mathbf{x}(0) \in U$, then the distance from $\mathbf{x}(t)$ to $\mathbb{A}$ tends to zero as $t \longrightarrow \infty$. This means that $\mathbb{A}$ attracts all trajectories that start sufficiently close to it. The largest U is called the basin of attraction of $\mathbb{A}$.
3. $\mathbb{A}$ is minimal: there is no proper subset of $\mathbb{A}$ that satisfied conditions 1 and 2.

In dynamical we can identify four types of attractors:

- The stationary attractor, which is a stationary point in the phase space, meaning that the state of the system is independent of time.
- The periodic attractor which is a close trajectory in the phase space indicating that the state of the system varies periodically with time.
- The quasi-periodic attractor which is a torus in the space phase indicating that the state of the system varies quasi-periodically at two (or three) incommensurable frequencies.
- The strange attractor which is a fractal, a geometrical object having infinite area and zero volume and folded infinite times in the phase space, indicating that the state of the system varies with time non-periodically.

The variable **x** varies over the phase space M, which is $\mathbb{R}^n$. If M is a linear space, we define the linear operator $D_x\phi^t$, matrix of partial derivates of ϕ at **x** (or a bounded operator if M is a Banach space). Let **P** be a fixed point for our dynamical system, i.e. $\phi^t\mathbf{P} = \mathbf{P}$ for all t. The derivative $D_P\phi^1$ of ϕ^1 (time-one map) at the fixed-point **P** is an nxn matrix or an operator in Hilbert space. When the time evolution id defined by the differential equation (2.3) in $\mathbb{R}^n$, the attractiveness condition is that the eigenvalues of Jacobian $\mathbf{J} = D_P\mathbf{F}$ all have a negative real part. In this case, the fixed-point **P** represents a stable equilibrium solution (attractors). An equilibrium is defined to be stable if all sufficiently small disturbances away from it damp out in time. Conversely, unstable equilibria , in which disturbances grow in time, are represented by unstable fixed point. A condition that occurs when at least one eigenvalue of the Jacobian matrix ***J*** has a positive real part.

Lorentz system (2.7) has two types of fixed points. The origin $(x^*, y^*, z^*) = (0,0,0)$ (Corresponds to a state of no convection (still air)) is a fixed point for all values of the parameters. For ρ>1, there is also a symmetric pair of fixed point $x^* = y^* = \pm\sqrt{\beta(\sigma-1)}$, $z^* = \sigma - 1$. Lorentz called them C^- and C^+.They represents left- or right-turning convection rolls (stationary air rotation). For 0<ρ<1 the origin is the only fixed point and is stable. Instead, for ρ>1 the origin becomes unstable and the two new points C^- and C^+ become stable for a $1 < \rho < \rho_H$, where the solutions of the characteristic equation for the eigenvalues of the Jacobian matrix in C^- and C^+ give to ρ_H equal to $\sigma(\sigma+\beta+3)/(\sigma-\beta-1)$ (assuming also that σ-β-1>0).

For a continuous-time dynamical system, suppose that there are a point **A** and a T>0, such that $\phi^T\mathbf{A} = \mathbf{A}$ but $\phi^t\mathbf{A} \neq \mathbf{A}$ when 0<t<T. Then **A** is a periodic point of period T, and therefore we will have that $\Gamma = \{\phi^t\mathbf{A}: 0 \leq t < T\}$ is the corresponding periodic orbit (or closed orbit). The attracting character of a periodic orbit may be studied with the help of Poincaré section.

Close orbits are not possible for a gradient system $\dot{\boldsymbol{x}} = -\nabla V$, for some continuously differentiable, single-valued scala function $V(\boldsymbol{x})$.

In fact: Suppose there were a closed orbit. We obtain a contradiction by considering the change in V after one circuit. On the one hand, $\nabla V = 0$ since V is single valued. But on the other hand,

$$\nabla V = \int_0^T \frac{dV}{dt}\, dt = \int_0^T (\nabla V \cdot \dot{\boldsymbol{x}}) dt = -\int_0^T ||\dot{\boldsymbol{x}}||^2 dt < 0$$

(Unless $\dot{\boldsymbol{x}} \equiv 0$, in which case the trajectory is a fixed point, not a closed orbit). This contradiction shows that closed orbit can't exist in gradient system.

The motion (by proper choice of coordinate φ) on a periodic orbit for a continuous system may be written $\varphi(t) = \varphi(0) + \omega t \ \ (mod\ 2\pi)$, where $\omega = 2\pi/T$. This may be thought of as representing the time evolution of a simple oscillator. Consider now a collection of k oscillators with frequencies $\omega_1, \ldots, \omega_k$ (without rational relations between the ω_i: no linear combination with nonzero integer coefficient vanishes). The motion of the oscillators is described by $\varphi_i(t) = \varphi_i(0) + \omega_i t \ \ (mod\ 2\pi)$, i=1,….,k, and this motion takes place on the product of k circles, (k>1), which is a k-dimensional torus T^k. Suppose that the torus T^k is embedded in $\mathbb{R}^n$ (n≥k); suppose, furthermore, that this torus is an attracting set. Then T^k is a quasi-periodic attractor. Quasi-periodic attractors are a natural generalization of periodic orbits, and they occur fairly frequently in the description of moderately excited physical systems.

Lorentz equations (2.7) do not have quasi-periodic solutions. We give a proof by contradiction. If there were a quasi-periodic solution, it would have to lie on the surface of a torus, and this torus would be invariant under the flow. Hence the volume inside the torus would be constant in time. But this contradicts the fact that all volumes shrink exponentially fast.

We have discussed attractors of dimension 0 (points) and dimension 1 (limiting cycle). However, in many situations the shape of the attractor is very complicated, and its dimension is not even integer. They are called fractals or strange attractor. For the common choice of the constants σ = 10, ρ = 28 and β = 8/3 ($\rho_H \approx 24.74\,, \varrho > \varrho_H$) the Lorentz system (2.7) exhibits both sensitive dependent on initial conditions behaviour and a fractal attractor with the typical butterfly shape in Figure 2.2.

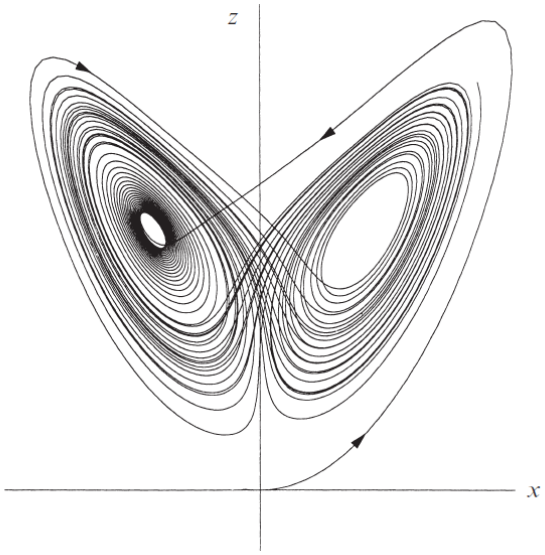

Figure 2.2 Lorent 63 attractor. From Nonlinear Dynamics and Chaos. *CRC Press, second edition, 2015.*

A qualitative change in the dynamics which occurs as a system parameter varies is called bifurcation. In particular, fixed point can be created or destroyed, or their stability can change. The parameter values at which they occur are called bifurcation points.

Let us briefly mention an overview of the main types of bifurcations:

- Saddle Point Bifurcation: Two equilibrium points, one stable (node) and one unstable (saddle), approach each other, collide and annihilate each other as the parameter varies.
- Transcritical Bifurcation: Two equilibrium points collide and exchange their stability, but do not disappear.
- Pitchfork Bifurcation: Typical of systems with symmetry. A fixed-point changes stability and generates two others, symmetrical to the first. It can be supercritical (stable becomes unstable, two stable points are created) or subcritical (unstable becomes stable, two unstable points collide).
- Hopf bifurcation: A fixed-point changes stability (going from stable to unstable or vice versa) and generates a periodic solution (limit cycle). It can be supercritical (stable) or subcritical (unstable).
- Period-doubling bifurcation: A limit cycle becomes unstable and generates a new cycle with double the period.

Summarizing what we have seen with the Lorenz system (2.7), we have that as the parameter ρ (which represents thermal thrust) varies, the system undergoes several bifurcations.

- $0<\rho<1$: Fixed point at origin. For low heat values, the air remains still. The only stable state is the absence of convection.
- $\rho=1$: Pitchfork Bifurcation. The origin loses stability, and two new stable equilibrium points arise, representing constant convection (clockwise or counterclockwise).
- $\rho = \rho_H$ (usually designed for $\rho_H \approx 24.74$, common choice of the constants $\sigma = 10$, $\rho = 28$ and $\beta = 8/3$) : Hopf bifurcation. Stable equilibrium points become unstable. The system can no longer stabilize itself in constant motion and begins to oscillate.
- $\rho > \rho_H$ (typically studied at $\rho = 28$): The system exhibits the so-called "butterfly effect": tiny variations in initial conditions lead to completely different results over time (making long-term weather forecasts inherently impossible), giving rise to a famous strange attractor called the Lorentz attractor.

2.3 Dimensions

The peculiarity of dynamical systems is the fact the typically their attractors have a dimension that cannot be described by an integer value: they are thus fractals, a term first coined by (Mandelbrot, 1982) who first started systematically studying the geometric properties of those objects. Fractals exhibit a fine structure at arbitrary small scale, and the determination of their dimension can provide information on the mathematical space needed to describe such objects.

To study attractors in the point of view of geometry , one must measure the dimension of those geometrical objects to find the difference in the dimension for various attractors. The dimensions of a geometric object can be defined in many ways. Among the most famous we have the Hausdorff dimension D_H, the capacity dimension D_C, and D_q dimension.

Capacity dimension can be introduced in an intuitive manner as an extension of integer dimension of simple shapes such as lines, squares, cubes, and spheres. Namely, suppose S is some smooth manifold embedded in $\mathbb{R}^n$of dimension $1 \leq D \leq n$, necessarily an integer, and $N(\epsilon)$ is the minimum number of volume elements (boxes, balls, etc.) in $\mathbb{R}^n$ of diameter $\epsilon > 0$ required to cover S, then $N(\epsilon) \propto \epsilon^{-D}$ for some real k>0 we have $N(\epsilon) = k\epsilon^{-D}$.
If we take the logarithm,

$$\ln N(\epsilon) = -D \ln \epsilon + \ln k \quad \Longrightarrow \quad D = \lim_{\epsilon \longrightarrow 0^+} \frac{-\ln N(\epsilon) + \ln k}{\ln \epsilon} = -\lim_{\epsilon \longrightarrow 0^+} \frac{\ln N(\epsilon)}{\ln \epsilon}$$

and, as a result, motivates the following definition.

Suppose $S \subset \mathbb{R}^n$ is bounded and $N(\epsilon)$ is the minimum number of balls of diameter ϵ needed to cover S. Then the capacity dimension of S may be defined as

$$D_C = -\lim_{\epsilon \longrightarrow 0^+} \frac{\ln N(\epsilon)}{\ln \epsilon} \tag{2.8}$$

From this reasoning, it is easy to see that the dimension of a point is zero, and that of a line is one. . The capacity dimensions of those familiar geometrical entities are the same as those obtained empirically, i.e., they are all positive integers. But D_C is not necessary an integer from the definition of (2.8). For object called fractals, D_C can be a positive fraction or an irrational number.

This is because if we consider a strange attractor, which is a fractal object that we assume to be sensitive to initial conditions, the phase volume will expand infinitely in certain directions due to the divergence of trajectories caused by sensitivity to initial conditions. On the other hand, the phase volume will shrink to zero because the system is dissipative. In this paradoxical case, the phase volume can only satisfy both requirements by stretching and bending an infinite number of times. Therefore, the strange attractor is a complex geometric object with zero volume and infinite area. It is neither a solid nor a surface. Its dimension can only be a fraction between the dimensions of a solid and a surface.

The capacity dimension of the Lorenz attractor, calculated for the classical parameters (σ =10, ρ = 28, β = 8/3) is estimated to be around 2.06±0.01.

The Capacity dimension is constructed by observing the number of balls covering an attractor. But a trajectory may spend more time in one ball than in another, and this is particularly true for fractal attractors, so we would like not all balls to count equally, but to be weighted according to the frequency with which trajectories visit the various balls covering the attractor. We define these frequencies as natural if independent of the initial condition, except for a Lebesgue null measure set, and they are defined as

$$\mu_i = \lim_{T \longrightarrow \infty} \frac{\eta(C_i, \boldsymbol{x}_0, T)}{T} \tag{2.9}$$

where $\eta(C_i, \boldsymbol{x}_0, T)$ is the total duration of time spent by an orbit originating at $\boldsymbol{x}_0$ during the period T in ball C_i.
In 1983 Grassberger, Hentshell and Procaccia gave another definition of dimension, that generalized the Capacity dimension called D_q dimension.

$$D_q = \frac{1}{1-q} \lim_{\epsilon \longrightarrow 0} \frac{\ln I(q,\epsilon)}{\ln(1/\epsilon)} \qquad \text{where} \quad I(q,\epsilon) = \sum_{i=1}^{N(\epsilon)} \mu_i^q . \tag{2.10}$$

In which $N(\epsilon)$ is the number of balls of diameter ϵ needed to cover attractor. This definition depends on a continuous parameter q, which weights each volume element based on the frequency with which it is visited. If q=0 $I(q,\epsilon) = N(\epsilon)$ and therefore D_0 is equal to D_C.
By defining, $D_1 = \lim_{q\to 1} D_q$, from L'Hôpital's rule we get

$$D_1 = \lim_{\epsilon\to 0} \frac{\sum_{i=1}^{N(\epsilon)} \mu_i \ln \mu_i}{\ln(\epsilon)} \quad . \tag{2.11}$$

The quantity (2.11) is known as information dimension (Balantoni and Renyi, 1956). A property of D_q is that they generally decrease with increasing q, expect for the cases when $\mu_i \sim 1/N(\epsilon)$, in this case $D_q = D_0$.

2.4 Lyapunov Exponent

As mentioned before, a strange attractor in a dissipative system has two main characteristics. One is its sensitivity to initial conditions. The other is its fractal structure. The former describes the informative property of the system and is closely related to Lyapunov exponent and entropy. The latter describes the geometry of the system and is closely related to fractal dimension. These two properties and three relative characteristic quantities are the main basis of the study of the predictability theory.

Start by considering the following dynamic system,

$$\frac{\mathrm{dx_i}}{\mathrm{dt}} = \mathrm{F_i}(\mathrm{x_1}, \ldots, \mathrm{x_n}; \alpha) \qquad \mathrm{i} = 1,2, \ldots \mathrm{n} \tag{2.12}$$

where t is time, $\{x_i: i = 1, \ldots, n\}$ is a n-dimensional phase space, F_i is a n-dimensional vector which describes a velocity field, α is controlling parameter of the system which determines the type of attractors in the phase space. Assuming that Eq. (2.12) is a dissipative system, i.e. $\nabla \cdot \mathbf{F} < 0$.

One sign of the sensitivity of the system to the initial value is the rapidly increase of initially introduced errors with time. If the error of the system at time t is expressed as $\{\delta x_i: i = 1, \ldots, n\}$, then the following equation may be derived from (2.12),

$$\frac{d\delta x_i}{dt} = \sum_{j=1}^{n} J_{ij}\, \delta x_j \quad \text{where} \quad J_{ij} = \frac{\partial \mathrm{F_i}(\mathrm{x_1},\ldots,\mathrm{x_n},\alpha)}{\partial \mathrm{x_j}} \tag{2.13}$$

where $[J_{ij}]$ is the Jacobi matrix. The space formed by the error δx_i $(i = 1,..n)$ is called tangent space.

Let us assume $\boldsymbol{y}_0$ be an initial condition and $\boldsymbol{y}_m$ $(m = 0,1,..)$ the corresponding orbit. If we consider an infinitesimal displacement $\delta \boldsymbol{y}_0$ from $\boldsymbol{y}_0$, we will have that the evolution of a tangent vector will be given by

$$\delta \boldsymbol{y}_{m+1} = \boldsymbol{J}(\boldsymbol{y}_m) \cdot \delta \boldsymbol{y}_m \tag{2.14}$$

which determines the evolution of the infinitesimal displacement of the orbit from unperturbed orbit $\boldsymbol{y}_m$. In particular, $\delta \boldsymbol{y}_m / |\delta \boldsymbol{y}_m|$ gives the direction of the infinitesimal displacement and $|\delta \boldsymbol{y}_m|/|\delta \boldsymbol{y}_0|$ is the factor by the which the infinitesimal displacement grows. From (2.22), we can write:

$$\delta \boldsymbol{y}_m = \boldsymbol{J}(\boldsymbol{y}_{m-1}) \cdot \boldsymbol{J}(\boldsymbol{y}_{m-2}) \cdot \ldots \ldots \boldsymbol{J}(\boldsymbol{y}_0) \cdot \delta \boldsymbol{y}_0 = \boldsymbol{J^m}(\boldsymbol{y}_0) \cdot \delta \boldsymbol{y}_0 \tag{2.15}$$

Let us define the exponent Lyapunov for the initial conditions $\boldsymbol{y}_0$ and the initial orientation given by $\boldsymbol{u}_0 = \delta\boldsymbol{y}_0/|\delta\boldsymbol{y}_0|$ as

$$\lambda(\boldsymbol{y}_0, \boldsymbol{u}_0) = \lim_{m\to\infty} \frac{1}{m} \ln \frac{\|\delta \boldsymbol{y}_m\|}{\|\delta \boldsymbol{y}_0\|} = \lim_{m\to\infty} \frac{1}{m} \ln \|\boldsymbol{J}^{\boldsymbol{m}}(\boldsymbol{y}_0) \cdot \boldsymbol{u}_0\| \tag{2.16}$$

If the dimension of the map is N, then there will be N or less distinct Lyapunov exponents. We are interested in the limit, so we write:

$$\lambda(\boldsymbol{y}_0, \boldsymbol{u}_0) = \lim_{m\to\infty} \frac{1}{m} \ln \|\boldsymbol{J}^{\boldsymbol{m}}(\boldsymbol{y}_0) \cdot \boldsymbol{u}_0\| = \lim_{m\to\infty} \frac{1}{2m} \ln |\boldsymbol{u}_0{}^{\intercal} \cdot \boldsymbol{T}_m(\boldsymbol{y}_0) \cdot \boldsymbol{u}_0| \tag{2.17}$$

where $\boldsymbol{T}_m(\boldsymbol{y}_0) = \boldsymbol{J}^{\boldsymbol{m}}(\boldsymbol{y}_0)^{\intercal} \boldsymbol{J}^{\boldsymbol{m}}(\boldsymbol{y}_0)$ and $\intercal$ denote the transpose. Since $\boldsymbol{T}_m(\boldsymbol{y}_0)$ is a real nonnegative Hermitian matrix , its eigenvalue are real .
The analysis of the latter limit (2.17) relies on the Oseledet's Multiplicative Ergodic Theorem (1968), for which the limit

$$\boldsymbol{T}_m(\boldsymbol{y}_0) = \lim_{m\to\infty} [\boldsymbol{J}^{\boldsymbol{m}}(\boldsymbol{y}_0)^{\intercal} \boldsymbol{J}^{\boldsymbol{m}}(\boldsymbol{y}_0)]^{\frac{1}{2m}} \tag{2.18}$$

exists and depends on the initial condition $\boldsymbol{y}_0$. However, $\boldsymbol{T}_m(\boldsymbol{y}_0)$ can be diagonalized as

$$\boldsymbol{T}_m(\boldsymbol{y}_0) = \boldsymbol{P}_{\boldsymbol{y}_0} \boldsymbol{D} \boldsymbol{P}_{\boldsymbol{y}_0}{}^{\intercal} \tag{2.19}$$

where $\boldsymbol{P}_{\boldsymbol{y}_0}$ is the matrix of the orthonormal eigenvectors. The eigenvalue matrix $\boldsymbol{D}$ is not dependent anymore on the initial condition and the Lyapunov exponents in descending order $\lambda_1 \geq \lambda_2 \geq \cdots \lambda_n$ are the natural logarithms of its diagonal elements

$$\lambda_i = \ln \boldsymbol{D}_{ii} \tag{2.20}$$

Thus, we can speak of the Lyapunov exponents of an attractor without reference to a specific initial condition. The Lyapunov exponents arranged in an order from the largest to the smallest are called the spectrum of the Lyapunov exponents.

No definition of the term chaos is universally accepted yet, but, usually, an attractor is defined chaotic if it has a positive Lyapunov exponent. In this case typical, infinitesimally displaced, initial conditions separate from each other exponentially in time, with the infinitesimal distance between them on average growing as $exp(m\lambda_i)$.

Now, let us follow the temporal variation of an infinitesimal ball of diameter ε_0. As values and signs of the eigenvalue vary, the volume stretches or contracts at difference rates in different directions. Therefore, after a period, the ball will change to an ellipsoid of decreasing volume. The exponential increasing rate in different directions in the tangent space after long enough time T may be expressed by the average change of length $\varepsilon_i(T)$ of the basic axis relative to the initial diameter ε_0 of the ball as follows,

$$\lambda_i \approx \frac{1}{T} \ln \left(\frac{\varepsilon_i(T)}{\varepsilon_0} \right) \tag{2.21}$$

Lyapunov exponents are also useful to compute along the dimension of the attractor. Let K be the largest integer such that the sum of the K largest Lyapunov exponents is greater or equal to zero,

$$\sum_{j=1}^{K} \lambda_j \geq 0 \tag{2.22}$$

Define the quantity D_L called the Lyapunov dimension (Kaplan and Yorke 1979),

$$D_L = K + \frac{1}{|\lambda_{K+1}|}\sum_{j=1}^{K}\lambda_j \tag{2.23}$$

The conjecture states that Lyapunov dimension is equal to information dimension, at least for typical attractors

$$D_L = D_1. \tag{2.24}$$

The practically most important parameters are λ_1 (maximum exponent) and $\sum\lambda_i(\lambda_i > 0)$. The former is a good criterion for chaotic behaviour; the latter describes the average exponential increase rate of an infinitesimal volume in its expanding direction in the phase space. As both can describe quantitatively the amplifying rate of chaotic system versus the initial uncertainty, they can be used as a 'ruler' for measuring the predictability of a generic state of the system.

2.5 Ergodicity

Dynamic systems in which the temporal evolution visits the entire phase space are called ergodic. Ergodic systems are of considerable interest because the averages of the set can be calculated using time averages, thus greatly simplifying the calculation. The problem of assessing whether a system satisfies the ergodic hypothesis is known as the modern ergodic problem.

Let us consider the triple (Γ, f^t, μ), where respectively Γ is the phase space, f^t is the time evolution operator and μ is an invariant measure under evolution of the time operator f^t, i.e.,

$$\boldsymbol{x}_0 \longrightarrow \boldsymbol{x}_t = f^t x_0 \qquad\qquad \mu(B) = \mu(f^{-t}B),$$

for any measurable set $B \subset \Gamma$.

A system (Γ, f^t, μ) is said ergodic , with respect to the invariant measure μ, it for any integrable function $O(\boldsymbol{x})$, we have

$$\bar{O} := \lim_{T\longrightarrow\infty}\frac{1}{T}\int_{t_0}^{t_0+T} O(\boldsymbol{x_t})dt = \int_{\Gamma} O(x)d\mu(\boldsymbol{x}) =: \langle O\rangle_{\mu} \tag{2.25}$$

where $\boldsymbol{x_t} = f^{t-t_0}\boldsymbol{x}_0$ for almost all initial condition $\boldsymbol{x}_0$.
We first remark that all the definitions are done with respect to the measure μ, thus possibly failing for sets for sets of zero μ measure, which are not null with respect to another measure.

2.6 Entropy

Besides Lyapunov exponents ad dimensions, there is another important characteristic quantity describing the information characteristics of dissipative system, i.e. the Kolmogorov-Sinai entropy or metric entropy. The metric entropy can be thought of as a number measuring the time rate of creation of information as a chaotic orbit evolve. This statement is to be understood in the following sense. Due to sensitivity to initial conditions, infinitesimally close trajectories diverge because of the positivity of the largest Lyapunov exponent (entropy is produced in the system). If we can only distinguish the initial positions in phase space with a certain degree of precision, then two orbits may initially appear to be the same. However, as the orbits evolve over time, they may drift apart and appear different. On the other hand, as an orbit is iterated, observing its position with the precision we have available, the initially insignificant digits in the specification of the initial condition will

eventually make themselves felt. So, assuming we can calculate accurately and know the dynamic equations that determine an orbit, if we observe that orbit with limited precision, we can, in principle, use our observations to obtain more information about the unresolved initial digits that specify the initial condition. In this sense, we can say that a chaotic orbit creates information.

Metric entropy is based on Shannon entropy, which measures the amount of information contained in a probabilistic event. Let $p_1, p_2, \dots, p_n$ a discrete probability distribution, i.e. $p_i \geq 0, \forall i$, and $\sum_{i=1}^{n} p_i = 1$. Shannon entropy id defined:

$$H_S(p_1, \dots, p_n) = -\sum_{i=1}^{n} p_i \ln p_i \tag{2.26}$$

where we define $p \ln p \equiv 0$ if $p=0$. For example, if one of the events was certain, i.e. $p_r = 1$ for a certain r and $p_i = 0$ for $i \neq r$, thus the information contained in that event would be zero $H_S = 0$. On the other hand, the case of maximum uncertainty will occur if all events have the same probability, i.e. $p_i = 1/n \ \forall i$, in this case (2.37) gives $H_S = \ln n$.

Let ρ an invariant measure for the dynamical system with compact support W. Let $\{W_i\}$ a partition into n disjoint components of W, we can define the entropy of partition as

$$H(\{W_i\}) = -\sum_{i=1}^{n} \rho(W_i) \ln[\rho(W_i)] \tag{2.27}$$

Now, let us build a sequence $\{W_i^m\}$ of smaller and smaller partitions by considering the sets $\phi^{-t}(W_i)$, i.e. the backward evolution of steps t = 1, 2, . . . , m of the partition set W_i . Then, for each pair of integer j and k (j, k =1,2,..,n) , we form n^2 intersections

$$W_j \cap \phi^{-1}(W_k),$$

and we say that all those nonempty intersections are the second partition $\{W_i^2\}$. Then next stage of partition $\{W_i^3\}$ is obtained by forming the n^3 intersections (j, k,l =1,2,..,n)

$$W_j \cap \phi^{-1}(W_k) \cap \phi^{-2}(W_l)$$

Therefore, at stage m, we have

$$\{W_i^m\} = \left\{W_{i_1} \cap \phi^{-1}\left(W_{i_2}\right) \cap \phi^{-2}\left(W_{i_3}\right) \cap \cdots\cdots \cap \phi^{-m+1}\left(W_{i_m}\right) \neq \emptyset \ : (i_1, i_2, . i_m) \in (1,2,\dots,n)\right\}$$

By taking the limit for $m \to \infty$ and the upper extreme over all possible partitions of the support of ρ, the metric entropy (density) of the invariant measure ρ is defined as

$$h(\rho) = \sup_{\{W_i\}} \lim_{m \to \infty} \frac{1}{m} H(\{W_i^m\}) \tag{2.28}$$

In general, there is an interesting bound proved by (Ruelle, 1978) connecting the metric entropy with the sum of positive Lyapunov exponents.

$$h(\rho) \leq \sum_{\lambda_i > 0} \lambda_i \tag{2.29a}$$

In many situations, the latter inequality (2.29a) is often an equality, as it was proven to hold more generally, by Pesin for typical Hamiltonian systems (Pesin, 1976).

$$h(\rho) = \sum_{\lambda_i > 0} \lambda_i \tag{2.29b}$$

Subsequently, equality (2.29b) was further generalised to the Axiom A attractors of dissipative dynamical systems (Ruelle, 1989). (An attractor is said to satisfy Axiom A if it is hyperbolic and if the periodic orbits are dense in the attractor).

2.7 Extreme Value Theory

Extreme value Theory was originally introduced by Fisher and Tippett and formalized by Gnedenko, who showed that the distribution of the maxima of an asymptotical large sample of independent identically distributed (i.i.d.) stochastic variables converges under very general conditions to a member of the so-called Generalised Extreme Value (GEV) distribution.

Let $X_0, X_1, \ldots, X_{m-1}$ a sequence of independent identically distributed variables with cumulative distribution function (cdf) $F(x) = P\{a_m(M_m - b_m) \leq x\}$ where a_m and b_m are normalizing sequence and $M_m = max\{X_0, X_1, \ldots, X_{m-1}\}$. Starting from general assumptions about the nature of the parent distribution of data, Gnedenko demonstrated that the asymptotic distribution of maxima belongs to a single family of generalizes distribution called GEV, the cdf of which can be expressed as:

$$F_{GEV}(x; \mu, \alpha, \kappa) = e^{-t(x)} \tag{2.30}$$

where
$$t(x) = \begin{cases} \left(1 + \kappa\left(\frac{x-\mu}{\alpha}\right)\right)^{-1/\kappa} & if\ \kappa \neq 0 \\ e^{-(x-\mu)/\alpha} & if\ \kappa = 0 \end{cases}$$

The expression (2.30) is valid for $1 + \kappa(x - \mu)/\alpha > 0$. Where we are $\mu \in \mathbb{R}$ (location parameter) and $\alpha > 0$ (scale parameter) which replace them as scale constants a_m and b_m. When $\kappa \longrightarrow 0$, the distribution corresponds to a Gumbel type (Type 1 distribution). When the index is positive, it corresponds to a Fréchet (Type 2 distribution) ; when the index is negative, it corresponds to a reversed Weibull (Type 3 distribution).

Let us define an exceedance as $z = X - T$, which measure by how much X exceeds the threshold T. As discussed above, under the same conditions under which the block maxima of the i.i.d. stochastic variables X obey the GEV statistics, and with the additional assumption of having Poisson exceedances, the Fisher-Tippett-Gnedenko theorem gives that the exceedances z are asymptotically distributed according to the Generalized Pareto Distribution (GPD):

$$F_{GPD}(z; \xi, \sigma) = \begin{cases} 1 - \left(1 + \frac{\xi z}{\sigma}\right)^{-1/\xi} & for\ \ \xi \neq 0 \\ 1 - \exp\left(-\frac{z}{\sigma}\right) & for\ \ \xi = 0 \end{cases} \tag{2.31}$$

where the range of z is $0 \leq z < \infty$ if $\xi \leq 0$ and $0 \leq z \leq \sigma/\xi$ if $\xi > 0$.
Given a dynamic system $(\Omega, \mathcal{B}, \nu, F)$, where Ω is the invariant set in $\mathbb{R}^d$, $\mathcal{B}$ is the Borel σ-algebra, $F: \Omega \longrightarrow \Omega$ is a measurable map and ν an F-invariant Borel measure. With the aim of adapting the extreme value theory to the study of dynamic systems, let us consider the stationary stochastic process,X_0, X_1, ..., defined as:

$$X_n(x) = g\big(dist(F^n(x), \Gamma)\big) \quad \forall n \in \mathbb{N} \tag{2.32}$$

where 'dist' denotes a distance in the ambient space Ω, Γ is a given point and g is an observable function. Defining $r = dist(x, \Gamma)$, we ask that $g = g(r)$ be such that it presents a maximum g_{max} for $r = 0$ (finite or infinite) and be monotonically decreasing. Once a threshold $T = T(r^*)$ has been defined, the exceedance above it is studied. Whenever the distance between the orbits of a dynamic system and Γ is smaller than r^*, we will have a so-called exceedance.

Therefore, following the definition given above, the exceedances is $z = g(r) - T$. Bayes' theorems allow as to say that:

$$P\big(r < g^{-1}(z+T)\big|r < g^{-1}(T)\big) = P\big(r < g^{-1}(z+T)\big)/P(g^{-1}(T)).$$

Wanting to express this in terms of an invariant measure of the system, given that an exceedance has occurred, we have that the probability $H_{g,T}$ of observing an exceedance of at least z is given by:

$$H_{g,T}(z) \equiv \frac{\nu(B_{g^{-1}(z+T)}(\Gamma))}{\nu(B_{g^{-1}(T)}(\Gamma))} \tag{2.33}$$

where B is an open ball centred in Γ. We observe that the value of the previous expression (2.33) is one if z is equal to zero, decreases monotonically with z, and vanishes when the radius is given by $g^{-1}(g_{max})$. To address the problem of the extreme, we must consider small radii. In this regard, we will assume the existence of the following limit:

$$\lim_{r\to 0} \frac{\log \nu(B_r(\Gamma))}{\log r} = D(\Gamma) \quad \text{, for } \Gamma \text{ chosen } \nu - \text{almost everywhere} \tag{2.34}$$

where $D(\Gamma)$ is the local dimension of the attractor. Therefore, we can rewrite (2.33),

$$H_{g,T}(z) \sim \left(\frac{g^{-1}(z+T)}{g^{-1}(T)}\right)^{D(\Gamma)} \tag{2.35}$$

Let us now replace g with specific observables $g_i, i = 1,2,3$:

$$g_1(r) = -\log(r) \tag{2.36}$$

$$g_2(r) = r^{-\beta} \tag{2.37}$$

$$g_3(r) = C - r^{-\beta} \tag{2.38}$$

where C is a constant and $\beta > 0 \in \mathbb{R}$. By choosing an observable of the form given by either g_1, g_2 or g_3, we derive as extreme value distribution law one member of the Generalised Pareto Distribution family given in Eq.(2.31). Results are detailed below:

- g_1- type observable:
$$\sigma = \frac{1}{D(\Gamma)} \qquad \xi = 0; \tag{2.39}$$
- g_2- type observable:
$$\sigma = \frac{T\beta}{D(\Gamma)} \qquad \xi = \frac{\beta}{D(\Gamma)}; \tag{2.40}$$
- g_3- type observable:
$$\sigma = \frac{(C-T)\beta}{D(\Gamma)} \qquad \xi = -\frac{\beta}{D(\Gamma)}\ . \tag{2.41}$$

The previous expressions show that there is a simple algebraic link between the parameters of the GPD and the local dimension of the attractor around the point Γ. We note that, as the parameter ξ is inversely proportionality to $D(\Gamma)$, if we analyse system of intermediate or high dimensionality, the distributions associated with observables g_2 and g_3 are indistinguishable from what we get from g_1.

We observe that this was achieved simply by assuming the existence of an invariant measure and the possibility to define a local dimension D around the point Γ of interest. This also shows that the statistic of extreme provides us with a new algorithmic tool for estimating the local fine structure of the attractor. We have only fixed a priori a value for threshold and the number of maxima necessary to construct statistics.

2.8 Instantaneous Dimensions

To investigate the predictability of a system of interest, as in the case of the atmosphere, the method for doing so is to look at the evolution of the system in phase space. In the space phase we identify a subset, namely a finite-size manifold of trajectories , called attractor, followed by the dynamical system over time and denoted by $x(t)$.

The origin of unpredictability can be attributed to an intrinsic stochastic nature of the system or ignorance of the current state of the system (provided that the states are not correlate) or of the dynamic rule controlling its evolution or from a combination of both. It has been established that even low-dimensional non-linear systems may be difficult to forecast if they exhibit an exponential divergence of close-by states. In such cases, unpredictability arises from our imprecise knowledge of the current state of the system. Previously, we identified two quantities to characterise the predictability of a system: the maximum Lyapunov exponent λ_{max} and the full Lyapunov spectrum. The existence of at least one positive Lyapunov exponent is the distinguishing feature of a chaotic dynamic system. Therefore, measuring predictability in a dynamic system can be reformulated as calculating the divergence of a system's trajectories over time.

It is important to emphasise that the Lyapunov exponents are average quantities, and the average is typically performed over a long trajectory. It follows that they are indicators of the global predictability of the system, where the term global refers to the average properties of the system, therefore to the average predictability of the system. Although the average predictability of the system may be useful as well as operational requirements and priorities, point to the need to investigate a local concept of predictability. In fact, the evolution of a dynamic system can be extremely dependent on its initial state. We therefore need to understand the system's predictability in a specific region of the phase space (we will refer to these local characteristics also as instantaneous, since they refer to a specific time). This notion has extreme relevance in context of weather prediction. Combing Extreme Value Theory and the Poincaré recurrence theorem, it is possible to introduce a novel framework to measure the local properties of dynamical systems (-Lucarini, Faranda et al. Extremes and Recurrence in Dynamical Systems. Pure and Applied Mathematics: A Wiley Series of Texts, Monographs and Tracts (Wiley, 2016)).

In particular, the quantities measured are the local dimension of dynamical system and their persistence at any point in time. Under the ergodic assumption , the Poincaré recurrence theorem guarantees that the system will visit an arbitrary small neighbourhood of any state repeatedly as time passes.

Set an arbitrary point $\Gamma = x(t = t_\Gamma)$ on a chaotic attractor, we want to consider the probability P that a trajectory $x(t)$ returns within a neighbourhood (a sphere) of Γ. To identify these, we define the observable function g:

$$g(x(t), \Gamma) = -\log\left(dist(x(t), \Gamma\right) \tag{2.42}$$

where dist, as previously stated, is a distance. The application of negative logarithm increases the discrimination of small values of $dist(x(t), \Gamma)$, and also implies that g is large when dist is small.

We therefore observe that demanding a trajectory $x(t)$ fall within a sphere centred at Γ is equivalent to having time series $g(x(t), \Gamma)$ above a threshold $s(q, \Gamma)$, where $s(q, \Gamma)$ is function of Γ and a chosen percentile q.
Therefore, the exceedances z, as previously defined, will be:

$$z(\Gamma) = g\big(\Gamma, x(t)\big) - s(q, \Gamma) \qquad \forall\, g\big(\Gamma, x(t)\big) > s(q, \Gamma) \tag{2.43}$$

According to extreme value theory, assuming the independence of the exceedance, the cumulative probability distribution $P(z, \Gamma)$ can only follow the exponential member of the generalized Pareto distribution (2.31), that is (Freitas-Freitas-Todd theorem, modified in Lucarini et al. Universal behaviour of extreme value statistics for selected observables of dynamical systems (2012)):

$$P(z, \Gamma) \sim exp\left(-\frac{z(\Gamma)}{\sigma(\Gamma)}\right) \quad . \tag{2.44}$$

The parameter $\sigma(\Gamma)$ depends on the state Γ and can be used to derive the local (instantaneous) dimension $d(\Gamma)$ around the point Γ. The local dimension $d(\Gamma)$ is given by:

$$d(\Gamma) = \frac{1}{\sigma(\Gamma)} \tag{2.45}$$

If this approach is iterated for several different Γ point, the attractor dimension is the obtained as:

$$D(\Gamma) = \overline{d(\Gamma)}, \tag{2.46}$$

where the overbar means averaging over all Γ.
The previous result is valid when point Γ is at a high or intermediate distance from the attractor or fixed point. In most natural systems, fixed point is unstable: a trajectory passing close to a fixed point spends a finite amount of time in its vicinity before leaving. Such time can be computed by introducing a further parameter in the previous law. This parameter is indicated with $\theta(\Gamma)$ and is such that:

$$P(z, \Gamma) \sim exp\left(-\frac{\theta(\Gamma)\, z(\Gamma)}{\sigma(\Gamma)}\right) \quad . \tag{2.47}$$

We can interpret $\theta(\Gamma)$ as the inverse of the mean residence time within the ball centred in Γ. The inverse of $\theta(\Gamma)$ is called persistence parameter. Since $0 < \theta(\Gamma) < 1$, low values correspond to high persistence of the trajectory in the neighbourhood of Γ, values close to one imply that the trajectory immediately leaves Γ.
As a result of what has been discussed so far, the parameter $\theta^{-1}(\Gamma)$ is defined as the persistence of the state Γ and consequently $\theta(\Gamma)$ is defined as the inverse of the persistence of state Γ.

Chapter 3

Data analysis

The first two chapters of this thesis discussed some characteristics of the Earth's atmosphere and dynamic systems, respectively. At the end of the first chapter, we encountered (1.4.5) the primitive equations, a system of nonlinear differential equations that describe the movements of fluids in the atmosphere. The atmosphere is therefore characterised by chaotic dynamics and large-scale recurring patterns. These two characteristics point to the existence of an attractor.

We encountered an example of this in the simple Lorentz atmospheric convention model (2.7). In fact, for certain parameter choices, if we plot the solutions (x(t),y(t),z(t)) in 3D space, we do not obtain a circle (stable state) or a line (periodic state), but a figure resembling butterfly wings, a strange attractor. The graphs show trajectories that orbit around two points, passing from one to the other in an unpredictable manner, but always remaining confined to a specific region of space.

The behaviour of the real atmosphere is much more complicated than that of the highly simplified model used by Lorentz in his experiments. Whether the Earth's climate exhibits such regime-like behaviour, with multiple "attractors", or whether it should be viewed as varying about a single state that varies in time in response to solar, orbital, volcanic, and anthropogenic forcing is a matter of ongoing debate.

The analysis of dynamic systems has led to the fundamental notion that atmospheric motions are chaotic and tend to stabilize on an attractor. It would seem to be a good idea to estimate the average size D (2.46) of the attractor. This would certainly provide information on the degrees of freedom sufficient to describe atmospheric circulation. However, D is an average value, while many climatic phenomena are linked to transient and metastable states of the atmosphere. These are states whose dynamic properties depend on instantaneous rather than average properties of the attractor. Such local properties are uniquely determined by two quantities: the local dimension d and the stability of the state measured by the inverse of persistence θ. Quantities introduced and described at the end of the second chapter (2.8).

As we have already seen d is a measurement of geometry of the trajectories in a small region of the system's phase space. It is therefore linked to the number of active degrees of the freedom that a system can explore locally, or alternatively to the way the system approaches and departs from a given state. The persistence, usually denoted with is inverse θ,is a measure of the persistence time of the system in the above-mentioned small region of the phase space. θ tends to be sensitive to small changes of the system. The local dimension d and the inverse persistence θ provide us with information about intrinsic predictability of the atmosphere in phase space.

It is likely that many quantities that define an atmospheric state (Pressure, Temperature...) can influence intrinsic predictability and therefore modify the values of the d and θ metrics according to their changes. However, as already mentioned, we intend to identify and quantify the possible influence of moisture transport on the intrinsic predictability of Mediterranean cyclones, particularly in the eastern Mediterranean, specifically in the region between latitudes 27.5N and 37.5N and longitudes 25E and 40E. Moisture transport is quantified using Integrated Vapour Transport (IVT) (1.5), defined as the horizontal advection of integrated vapour along the vertical.

The following paragraphs will therefore present the source and nature of the data provided, before proceeding with their analysis. This analysis will attempt to correlate the d and θ metrics on days when cyclones are present with the water vapour influx provided by the IVT on the same days

3.1 Data

We can divide the data provided into two groups: one consisting of two lists, or rather two Excel files, and another group derived from the download of data from the ERA5 dataset. The first list shows the start date of all cyclones that occurred in the geographical area in question between 1 January 1981 and 31 December 2018. In addition to this data, the following columns provide data on the duration of these weather events and their intensity (in the column labelled "group"). Cyclones are classified into three groups according to their intensity class: low, mid and high intensity precipitation event. To be precise, this list includes 200 low-intensity cyclones, 578 mid-intensity cyclones and, finally, 205 high-intensity cyclones. The cyclones are classified using the upgraded semi-objective synoptic classification algorithm (Alpert et all, 2004; Ludwing and Hochman, 2022). Specifically, the classification used the days of the year 1985 and the winters of 1991 and 1992, classified into regional weather types by expert meteorologists, as 'ground truth' (426 days). Then , it finds the minimum Euclidean distance between a day of interest and the ground truth. The day with the minimum distance is labelled a specific weather type. This classification represents the regional weather condition well (Hochman et al, 2018) and is based on daily mean surface air temperature a 2-m (T2m), Sea-Level-Pressure (SLP), and 500hPa geopotential height (Z500) fields from ERA5 reanalysis.

The second list contains the values for each day between the above-mentioned dates of the local metrics d and θ for various geopotential heights Z and for precipitation. The geopotential heights for which the values of the two metrics d and θ of the dynamic system are provided are Z1000 (1000 hPa), Z850 (850 hPa), Z700 (700 hPa), Z500 (500 hPa), Z300 (300 hPa) and Z200 (200 hPa).

Reanalysis programs reconstruct past atmospheric conditions by analysing historical and present observational data using advanced numerical models (Fujiwara et al., 2022). Their purpose is to create an accurate, high-resolution dataset covering several decades that can be used in atmospheric analysis. ERA5 is the latest global climate reanalysis from the ECMWF (European Centre for Medium-Range Weather Forecasts), providing hourly atmospheric, land surface and ocean data from 1940 to the present day, with a spatial resolution of 0.25°x0.25° (latitude and longitude), approximately 31 km and 137 vertical levels. ERA5 operates in collaboration with the Copernicus Climate Data Store (CDS) so that data is updated daily. The ERA5 dataset provides a wide range of atmospheric variables (temperature at 2 metres, total precipitation, wind speed and direction, sea level pressure and humidity, etc.). ERA5 operates in two 12-hour windows: the first window runs from 09:00 to 21:00 UTC, while the second covers the time interval from 21:00 to 09:00 UTC the following day. Observational data from various sources (including satellites, radiosondes, surface weather stations, aircraft and ships) are assimilated by ERA5 continuously, on an hourly basis, and nine hours after the start of each window, a short-term forecast is produced. This forecast is used together with the latest available information to update the initial conditions for the next cycle. ERA5 data are then made available to the public on the Copernicus Climate Data Store (CDS) website with a delay of five days from the current date.

Our aim was to obtain the values of the IVT vector for the period between 1 January 1981 and 31 December 2018 in the above-mentioned area of the eastern Mediterranean. To this end, the two components of the IVT vector, the eastward component (the zonal component) and the northward component (the meridional component), were downloaded from the Copernicus Climate Data Store website. This download took place at four different times each day between the two dates indicated above at various points evenly distributed throughout the region under consideration. For complete information, the four times each day, within the specified date range, at which the data was downloaded are precisely: 00:00, 06:00, 12:00 and 18:00. Furthermore, since the spatial resolution of the ERA5 data is 0.25°x0.25° (latitude and longitude), for each of these times, the values of the zonal

component of the IVT (IVTu) and the values of the meridional component of the IVT (IVTv) will each form a matrix of 41 rows by 61 columns.

3.2 Analysis

The first list provided the dates of each cyclone that occurred in the region under consideration, in the period between the dates indicated above, while the second list provided the values of the metrics d and θ for each day included in the period under consideration, in the same geographical region. Thus, to compensate for seasonal changes, the average values of the d and θ metrics were calculated for each of these days, starting from -W days to $+W$ days from the date of each cyclone. To perform these calculations, a programme was written in Matlab in which the parameter W can be entered as input. In our case, we opted for W=15 days. We would like to point out that Matlab was the tool used throughout the data analysis. These averages were then saved in an additional list.

The values of the metric parameters d and θ, referring to the initial date of each cyclone, subtracted from the average values calculated in this way, will constitute the values on the y-axis for the scatter plots subsequently produced. In Figure 3.1 shows, for cyclones of all intensity and for the geopotential height Z1000, the time series of the difference between the local dimension d on the day of the cyclone and the average $< d >$ calculated from 15 days before to 15 days after the date of each cyclone.

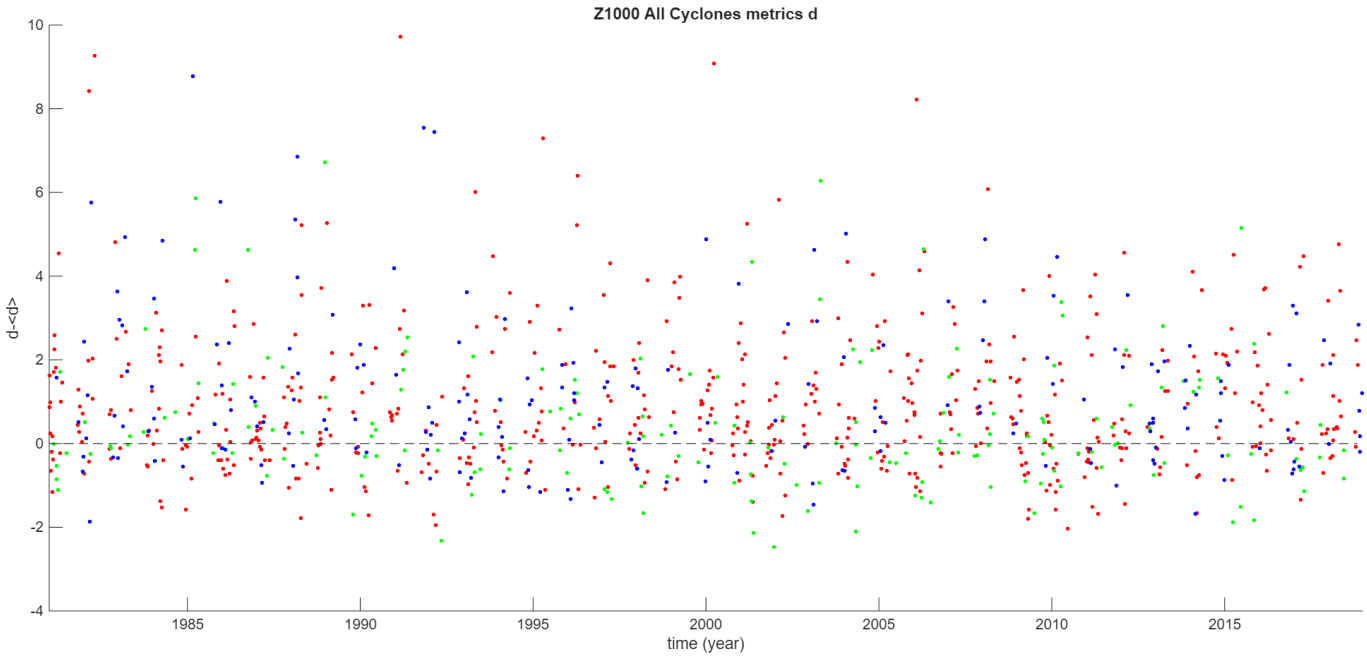

Figure 3.1-Time series of the instantaneous dimension d-<d> during the cyclones. (low-intensity cyclones are shown in green, mid-intensity cyclones are shown in red, and heavy-intensity cyclones are shown in blue).

Starting from the data downloaded from the ERA5 dataset, i.e. the value of the respective zonal and meridional components of the IVT vector, we proceeded to calculate the IVT vector magnitudes for each day and each of the four hours indicated above, at various points in the region of interest. The calculation was performed using equation (1.52). As previously specified, the region in question was divided into a grid with a step size of 0.25° latitude and 0.25° longitude (41X61 points). The values of the IVT vector module, as was done for the two components: IVTu (zonal component) and IVTv (meridional component), were saved in a 41x61x55516 matrix, where the indices between 1 and 41 refer to latitude values, the indices between 1 and 61 relate to longitude

values, and the indices between 1 and 55516 indicate the elapsed time. To be precise, each value in the third index of the matrix refers to the number of seconds elapsed between the date and time under consideration and 1 January 1970. Therefore, setting the third index equal to one will give us the data for 6 a.m. on 1 January 1981, while setting it equal to 55516 will give us the data for midnight on 31 December 2018.

At this point, an additional matrix was constructed by sorting the IVT amplitude matrix in ascending order along the third dimension. This was done to calculate various threshold values or percentiles. Using the knowledge of the length of the third dimension of the newly saved sorted matrix, the value of the percentile sought was multiplied by this length, thus setting a value in the third dimension and obtaining a 41x61 matrix. Proceeding in this way for multiple percentile values resulted in multiple matrices, which when combined allowed a matrix of percentiles to be obtained and saved. The tabulated percentiles of values: 0.75, 0.80, 0.85, 0.90 and 0.95. For our future investigations, a value of 0.85 has been chosen. The percentile in question is shown in Figure 3.2.

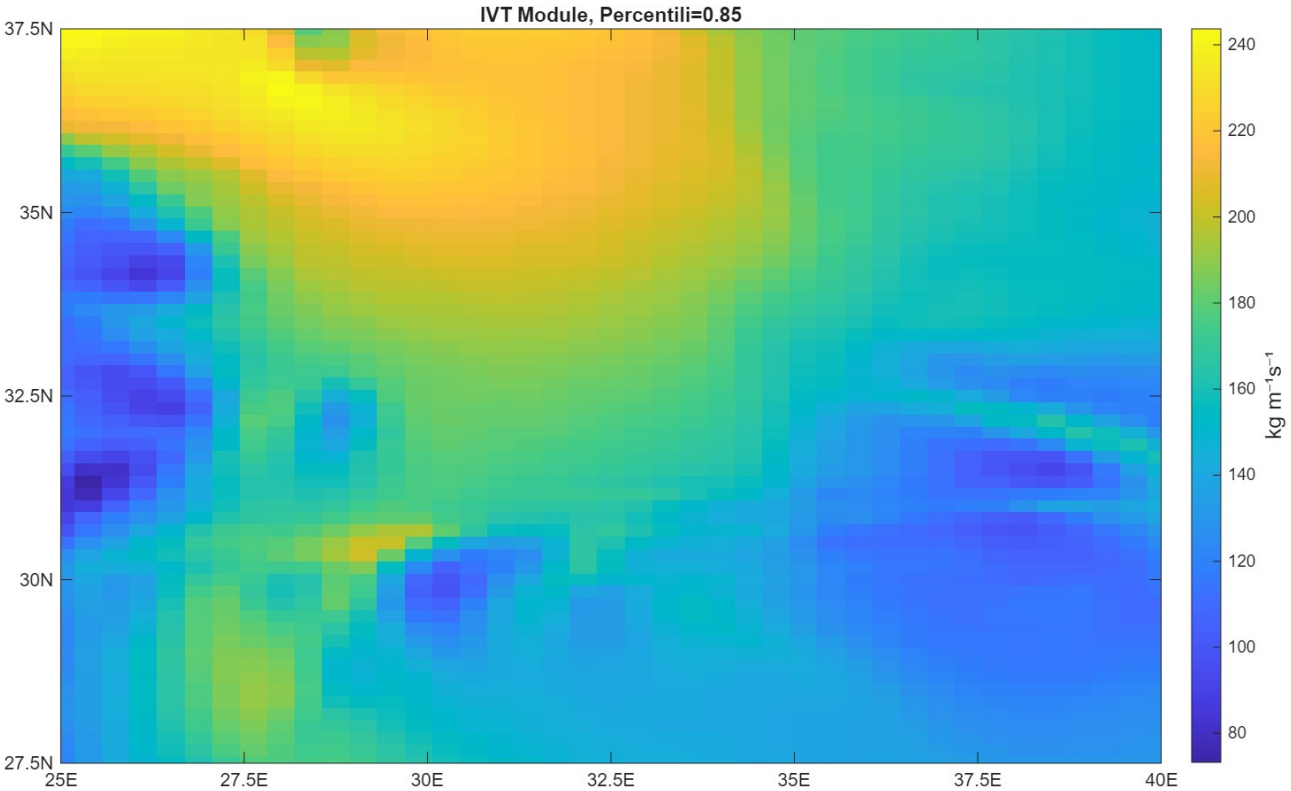

Figure 3.2-IVT amplitude-0.85 Percentile

The next step was to construct a binary matrix for each initial day of a cyclone, for the previous day, for two, for three and four days, plus the day the cyclone began, and for each of the four times, whose values were zero or one depending on whether the value in the corresponding matrix of IVT module point values exceeded the value in the percentile matrix. Further investigation of these binary matrices provided information on the regions (connected areas) where the IVT amplitude exceeded the set threshold value. More specifically, the following were calculated: the extension of each of the areas and the integral of the IVT module on each of these areas. Finally, the area of maximum extension and the maximum integral of the IVT were chosen as variables identifying a day or a group of days. All these values were then saved in an Excel file, to subsequently form the x-axis values for future scatter plots.

Having set a threshold, the number of cyclones that make up our sample has decreased. As expected, this occurred more frequently in low-intensity cyclones. . To be precise, this new list includes 183 low-intensity cyclones, 551 mid-intensity cyclones and, finally, 201 high-intensity cyclones.

Considering this selection, Figures 3.3-3.4 show the Boxplots between metrics d and θ on the day a cyclone began, subtracted from their averages and various geopotential height Z and precipitation.

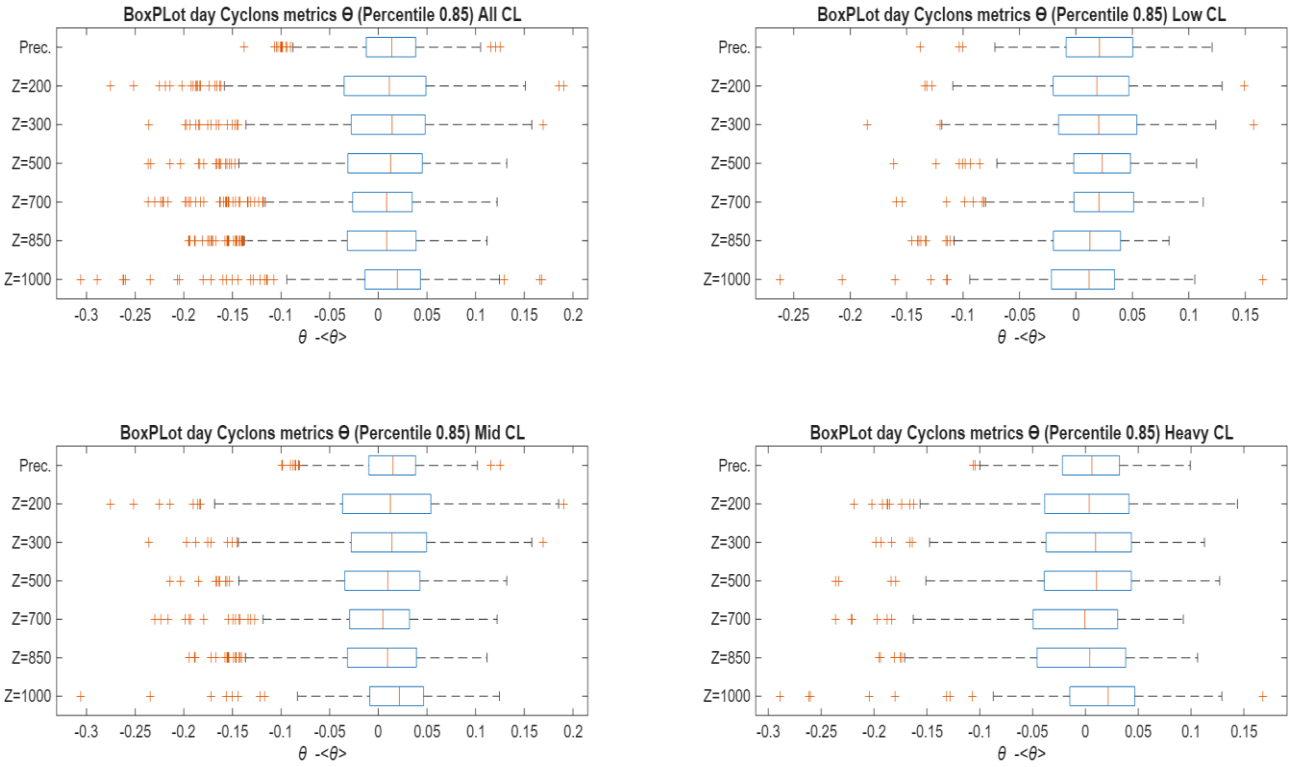

Figure 3.3-BoxPlot between metrics θ-<θ> and geopotential height Z and Precipitation

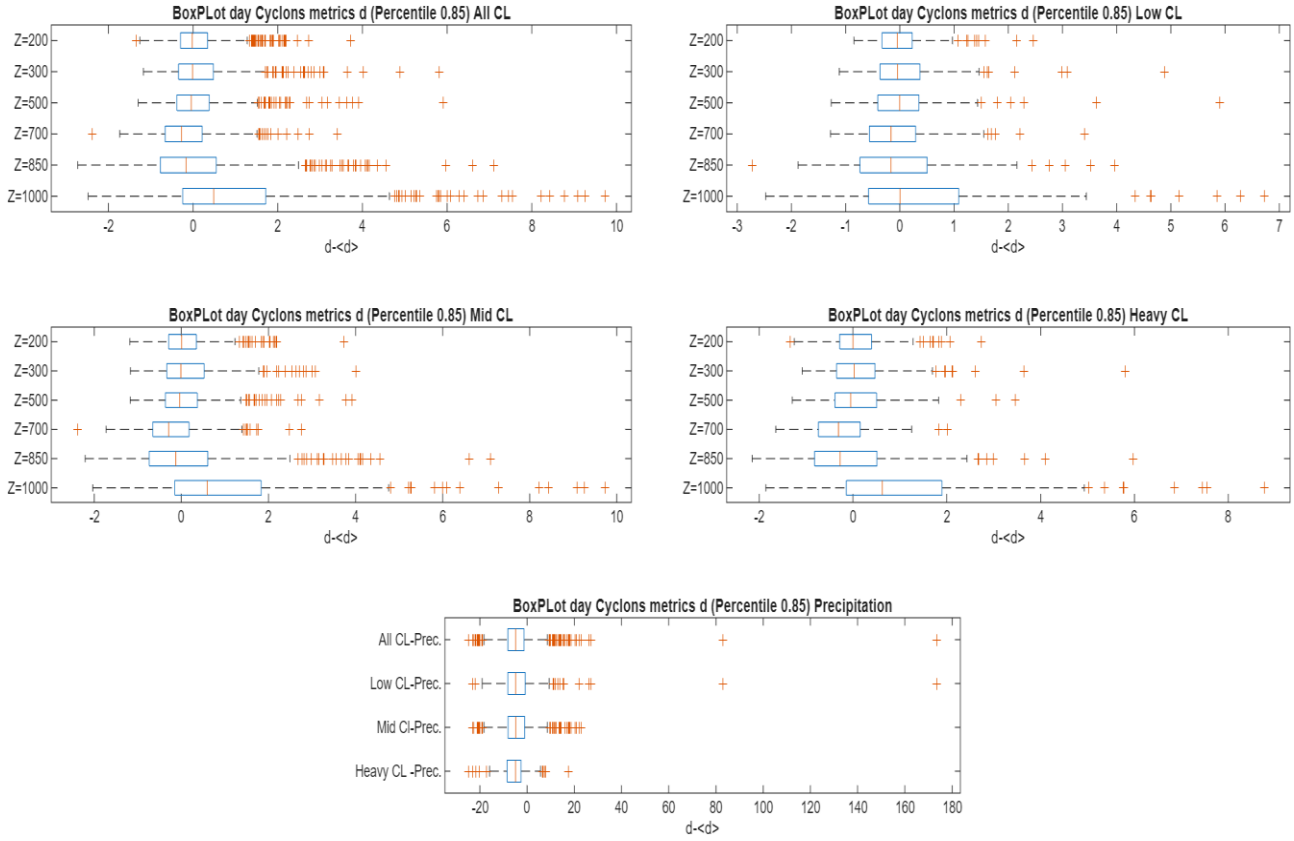

Figure 3.4 --BoxPlot between metrics d-<d> and geopotential height Z and precipitation

Boxplots are non-parametric graphic representations of data: they give a clear display of the spread of the data without making any assumption on their underlying statistical distribution. The principal elements of these graphs are:

- the median, here represented as an orange straight line.
- The boxes, in our case empty rectangles whose sides are drawn in blue, which contain the middle 50% of the statistical population. In fact, the right and left extremes of the boxes identify the 75th quartile and the 25th quartile, respectively. The length of the boxes, between the two quartiles , is called inter-quartile range (IQR).
- The lines extending from the box are called whiskers. Whiskers represent the expected data variation and extend 1.5 times the IQR from the right and left sides of the box (in our case). Data points that fall to the right or left of the end of the whiskers are represented as orange crosses, called outliers. An outlier is more extreme than the expected variation, but still statistically possible.

By looking at the two Boxplots, the local dimension d subtracted from its mean generally has outliers only on the right side, indicating that the right tail of the distribution is longer, indicating positive skewness. A generally opposite behaviour is shown by the inverse of the persistence θ. The behaviours observed for both metrics vary in intensity across all geopotential heights.

For each of the two variables identified for the x-axis: the area of maximum extension and the maximum integral of the IVT module, 210 scatter plots were created which, as already mentioned, presented the values of the d and θ metrics for the various geopotential heights and precipitation on the y-axis. An example is shown in the Figure 3.5, where it is displayed the situation on the day of onset for three classes of cyclones. Specifically, on the x-axis of the Figure 3.5, we have the maximum integral of IVT module, while on the y-axis we have the value of the local dimension d. Note that the same operation was also performed for the day before the start of the cyclone, for two, for three and for four days. This example was also included to show how scatter plots, in our case, are difficult to read, and how it is therefore necessary to represent our conclusions in a different way.

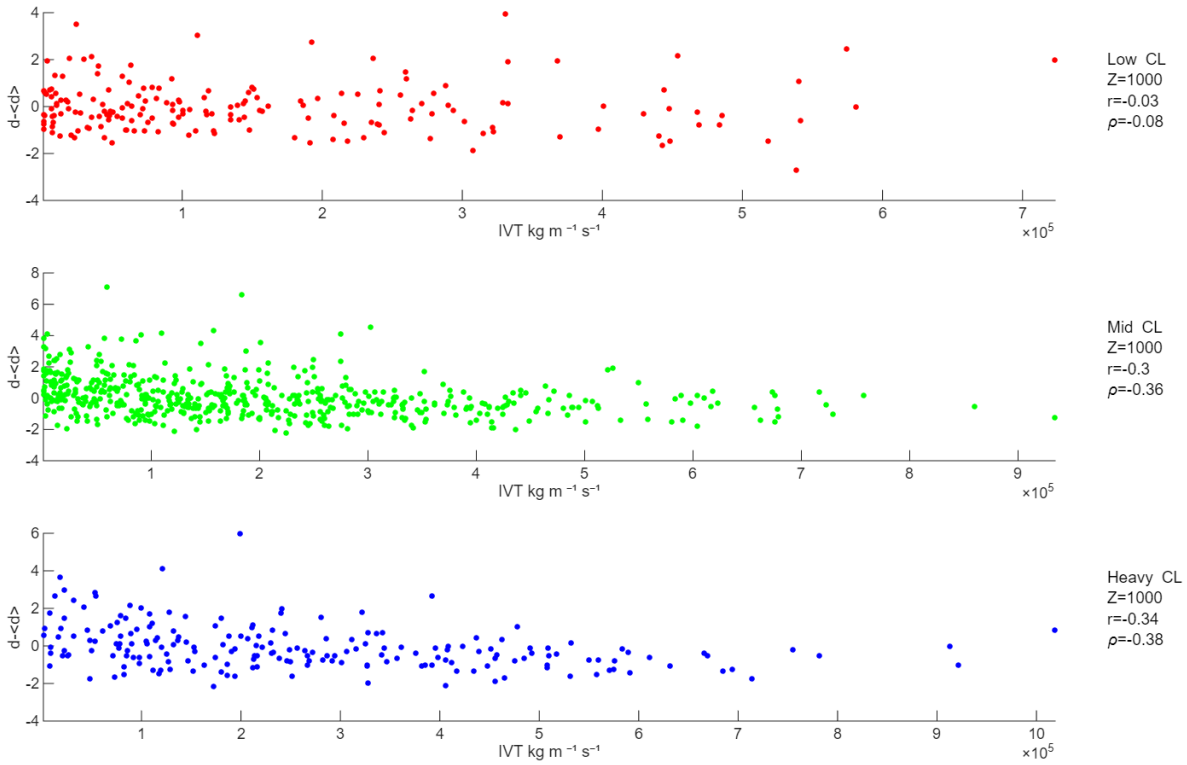

Figure 3.5 Scatter plots- (|IVT|, d-<d>)). Day when the cyclone begins

The aim is to identify and quantify the possible influence of moisture transport on the intrinsic predictability of Mediterranean cyclones, particularly in the eastern Mediterranean. Therefore, Pearson's correlation coefficient (indicated by r) and Spearman's correlation coefficient (indicated by ρ) were calculated for each pair of variables in these scatter plots. These values were in turn represented in graphs and, for better and more direct use, reported in tables. In the tables, the most significant correlation values were coloured once their possible significant difference from zero was identified using a permutation test. Two tables showing the correlation values for the local dimension d, for the day the cyclone began and for the day before it began, are shown in the Figure 3.6. The same information is shown in the two tables in the Figure 3.7, referring in this case to the inverse of the persistence θ.

	metrics d, Day the cyclon, Maximum integrated vector IVT module					
	Low CL		Mid CL		heavy CL	
	r	ρ	r	ρ	r	ρ
Z=1000	-0.0278	-0.0795	-0.2992	-0.3567	-0.3393	-0.3844
Z=850	0.2625	0.2733	0.0307	0.0464	0.0858	0.0114
Z=700	0.1946	0.1823	0.0945	0.0710	0.1330	0.1596
Z=500	0.1206	0.1192	0.0223	0.0478	0.0996	0.1012
Z=300	0.1601	0.1131	0.1055	0.1027	0.2970	0.2308
Z=200	0.0330	-0.0115	-0.0007	-0.0197	-0.1244	-0.1458
Prec.	-0.0269	-0.1219	-0.2597	-0.2867	-0.1324	-0.2058

	metrics d, Day before the cyclon, Maximum integrated vector IVT module					
	Low CL		Mid CL		heavy CL	
	r	ρ	r	ρ	r	ρ
Z=1000	-0.0224	-0.0485	-0.2659	-0.3284	-0.3400	-0.3760
Z=850	0.0645	0.0593	-0.0921	-0.1069	-0.0692	-0.1316
Z=700	0.1954	0.1634	0.0939	0.0523	0.0875	0.1031
Z=500	0.0872	-0.0044	-0.0137	0.0116	0.0136	0.0497
Z=300	0.1572	0.0833	0.0659	0.0752	0.1032	0.1253
Z=200	-0.0525	-0.1018	0.0379	0.0296	-0.0593	-0.0849
Prec.	-0.0748	-0.0653	-0.1504	-0.1749	-0.1022	-0.2032

Figure 3.6- Correlation tables between metric d and |IVT|

The permutation test is a nonparametric statistical method used to test the significance of the coefficients of a model when classical assumptions, such as normality, are not satisfied. In our case, we do not know the distribution followed by the data, and furthermore, the previous analysis of our data's Boxplots highlighted how their distribution was skewness, i.e., it presented outliers mainly in a single direction. These observations lead us to prefer the use of a permutation test to a t-test. In fact, the only assumption made is the possibility of permuting one of the two data sets for which the correlation coefficients have been calculated. It was decided to permute the variable on the x-axis,

i.e., the modulus of the IVT vector. One thousand permutations were performed, and the values of the Pearson and Spearman correlation coefficients were calculated for each of them.
Therefore, given a level of significance α. In our case, we set α equal to 0.05. We proceeded by verifying whether the Pearson and Spearman correlations calculated were greater than 95% of those calculated with reshuffling if positive, or less than 95% of those calculated with reshuffling if negative (Some tables showing the threshold values calculated with the permutation test can be found at the end of Appendix C for the local dimension d).
In the tables presented here, cells containing values that pass the permutation test are coloured cyan if the value is negative and green if positive.

	metrics θ, Day the cyclon, Maximum integrated vector IVT module					
	Low CL		Mid CL		heavy CL	
	r	ρ	r	ρ	r	ρ
Z=1000	-0.2107	-0.1052	0.0054	0.0828	-0.2033	-0.1134
Z=850	0.0073	0.0758	-0.0240	-0.0133	-0.1930	-0.0977
Z=700	-0.1428	-0.0343	-0.0292	0.0122	-0.0533	0.0187
Z=500	-0.0931	-0.0639	0.0184	0.0237	0.1698	0.2047
Z=300	-0.0326	-0.0177	0.1282	0.0969	0.1913	0.2128
Z=200	0.0033	-0.0028	0.0532	0.0316	0.1418	0.1025
Prec.	0.2757	0.2050	0.0605	-0.0309	0.0380	-0.0847

	metrics θ, Day before the cyclon, Maximum integrated vector IVT module					
	Low CL		Mid CL		heavy CL	
	r	ρ	r	ρ	r	ρ
Z=1000	-0.0849	-0.0237	0.0302	0.0733	-0.1355	-0.0785
Z=850	-0.0699	-0.0221	-0.0749	-0.0699	-0.1529	-0.1363
Z=700	-0.2007	-0.0943	-0.0309	-0.0118	-0.0540	-0.0110
Z=500	-0.1655	-0.0880	0.0074	0.0145	0.0915	0.1103
Z=300	-0.1282	-0.0648	0.0988	0.0747	0.0501	0.0858
Z=200	-0.0655	-0.0575	0.0526	0.0238	0.0568	0.0048
Prec.	0.2688	0.1216	0.1273	0.0739	0.0185	-0.1023

Figure 3.7- Correlation tables between metric ϑ and IVT

The tables relating to two, three and four days, plus the initial day of the cyclone, for the maximum integrated IVT and for the area of maximum extension, are shown in Appendix D.

The results, concerning the maximum integral of the modulus of the IVT vector, shown in the table in Figure 3.6, but also in all the others in the appendix, show that the correlation values for the local dimension d are negative for the geopotential height Z1000 and for precipitation, for all cyclone classes. These values are statistically significant for mid- and heavy-intensity cyclones near the ground, i.e. at geopotential height Z1000. This suggests the possibility that an increase in horizontal

moisture flow leads to a decrease in local dimension *d* and therefore to an increase in intrinsic predictability for the geopotential height Z1000.
On the contrary, the tables in Figure 3.7 do not provide us with any evidence that might suggest the existence of a monotonic relationship between the increase in horizontal moisture flux, represented by the IVT vector module, and the inverse of persistence θ.

The same series of operations and analyses was then carried out for the zonal component of the IVT (IVTu) and for its meridional component (IVTv) (we recall that we had two matrices of the values of IVTu and IVTv). The difference in this case is that the IVTu and IVTv can be either positive or negative. Recalling what was said in paragraph 1.2 regarding the conventions on the horizontal components of wind speed (u and v), IVTu will be positive if directed eastwards and negative if directed westwards, while IVTv will be positive if directed northwards and negative if directed southwards. Therefore, there were not two variables but four. The first operation was to achieve the percentiles. Starting from the IVTu and IVTv matrices, a pair of matrices was created by sorting the same matrices in ascending order, and another pair by sorting them in descending order. From the first pair, the percentiles for the positive components were obtained, and from the second pair, the percentiles for the negative components. The same percentile values as indicated above were calculated. The threshold to be used was chosen so that the values present were of the same sign. The value of 0.85 was chosen, except for the zonal component towards the west, where 0.95 was chosen. We then proceeded as before, constructing binary matrices and obtaining from them the area of maximum extension and the maximum integral value. Variables achieved for the positive and negative components of both IVTu and IVTv. Finally, scatter plots were created and tables showing the values of Pearson's and Spearman's correlation coefficients were obtained. Figures 3.8, 3.9, 3.10 and 3.11 show the tables with the correlation values (for the maximum integrated IVT), on the day the cyclone began, for the eastward component of the IVTu, the westward component of the IVTu, the northward component of the IVTv and the southward component of the IVTv, respectively. The tables in the following figures all refer to metric *d*.

	metrics d, Day the cyclon, Maximum integrated zonal component IVT (IVTu Eastward)					
	Low CL		Mid CL		heavy CL	
	r	ρ	r	ρ	r	ρ
Z=1000	-0.0330	-0.0938	-0.3034	-0.3723	-0.3746	-0.4350
Z=850	0.2169	0.2203	-0.0053	0.0119	-0.0204	-0.1332
Z=700	0.0866	0.1339	0.0436	0.0329	0.0292	-0.0093
Z=500	0.0152	0.0618	-0.0730	-0.0473	-0.0241	-0.0491
Z=300	0.0960	0.0752	0.0220	0.0152	0.1494	0.0849
Z=200	-0.0074	-0.0873	0.0404	0.0346	-0.0894	-0.1440
Prec.	-0.0012	-0.1313	-0.3084	-0.3483	-0.1413	-0.2570

Figure 3.8- Correlation tables between metric d and IVTu Eastward

	metrics d, Day the cyclon, Maximum integrated zonal component IVT (IVTu Westward)					
	Low CL		Mid CL		heavy CL	
	r	ρ	r	ρ	r	ρ
Z=1000	0.1868	0.1025	0.1021	0.1282	0.1110	0.1189
Z=850	0.2825	0.1187	0.2141	0.1080	0.2474	0.2723
Z=700	0.5281	0.2039	0.1515	0.0300	0.1537	0.2196
Z=500	0.3783	0.0545	0.1890	0.0720	0.0505	0.0978
Z=300	0.3153	0.0784	0.1345	0.0329	0.1073	0.1157
Z=200	-0.2000	-0.0869	-0.1421	-0.1620	-0.1121	-0.2279
Prec.	0.0462	0.1397	0.1206	0.1759	0.2541	0.2716

Figure 3.9- Correlation tables between metric d and IVTu Westward

	metrics d, Day the cyclon, Maximum integrated meridional component IVT (IVTv Northward)					
	Low CL		Mid CL		heavy CL	
	r	ρ	r	ρ	r	ρ
Z=1000	-0.1934	-0.1697	-0.2644	-0.2953	-0.2912	-0.2866
Z=850	0.0999	0.1044	0.0324	0.0803	0.1301	0.1160
Z=700	0.1095	0.0859	0.0633	0.0723	0.1507	0.2448
Z=500	0.0691	0.0347	0.0299	0.0345	0.1819	0.1814
Z=300	0.1828	0.1393	0.1239	0.1144	0.4053	0.3681
Z=200	-0.1242	-0.1710	-0.0288	-0.0771	-0.0992	-0.1302
Prec.	-0.0121	-0.1430	-0.1531	-0.1598	-0.1150	-0.0805

Figure 3.10- Correlation tables between metric d and IVTv Northward

	metrics d, Day the cyclon, Maximum integrated meridional component IVT (IVTv Southward)					
	Low CL		Mid CL		heavy CL	
	r	ρ	r	ρ	r	ρ
Z=1000	0.1745	0.1904	0.2101	0.1487	0.4154	0.3288
Z=850	0.2505	0.1791	0.1482	0.0727	0.1240	0.1127
Z=700	0.3447	0.1955	0.2612	0.2042	0.2574	0.2361
Z=500	0.3289	0.2233	0.3405	0.2953	0.2271	0.2399
Z=300	0.2290	0.1118	0.2776	0.2267	0.0992	0.0710
Z=200	0.3092	0.3364	0.0431	0.0080	-0.0574	-0.1065
Prec.	-0.0630	-0.0033	-0.0741	-0.0332	0.0252	0.0060

Figure 3.11 Correlation tables between metric d and IVTv Southward

As regards the components of the IVT vector, the tables shown in Figures 3.8 and 3.10 show results like those shown in the table in Figure 3.6 for the IVT module. The positive component of IVTu (towards the east) and the positive component of IVTv (towards the north) give results similar to each other and to those obtained previously for the module. This is not the case for the respective negative components of IVTu (towards the west) and IVTv (towards the south), as can be seen from Tables 3.9 and 3.11.
The tables shown in Figures 3.8, 3.9, 3.10 and 3.11 show how the various components of the IVT vector behave differently. To study these differences in behaviour, these components were compared with each other and with the IVT module itself. This comparison was carried out using histograms with the value of the IVT integral on the y-axis. This comparison also allows us to determine whether one of the various components is predominant. These histograms are shown in Figures 3.13, 3.14, 3.15 and 3.16.

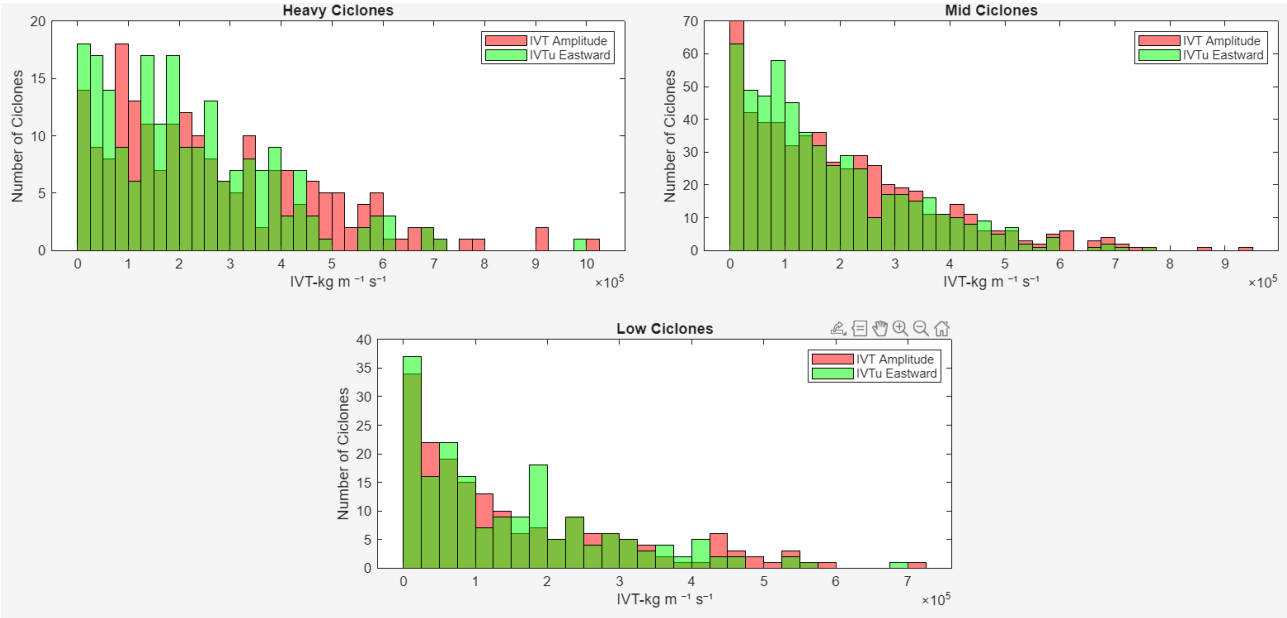

Figure 3.13- Histograms comparing the IVTu towards the East and the IVT Amplitude for the three cyclone classes.

Analysis of histograms (Figures 3.13, 3.14, 3.15 and 3.16) shows that the eastward zonal component is predominant, so much so that its distribution is like that of the module (Figure 3.13). The westward zonal component is of little significance as it is overshadowed by the eastward component (Figure 3.15). The southward component of IVTv compared with the eastward component of IVTu shows that the latter is predominant, although the IVTv component is not negligible and could have an effect if cyclones with strong southward winds are considered (Figure 3.14). In the case of the southward-directed IVTv component, the correlation values are positive, some significantly so (Figure 3.11). This suggests the possibility that an increase in southward horizontal moisture transport leads to an increase in the local dimension d and thus a decrease in intrinsic predictability.
The southern component of the IVT is balanced, with the northward thrust (positive IVTv) and southward thrust (negative IVTv) having similar distributions (Figure 3.16).

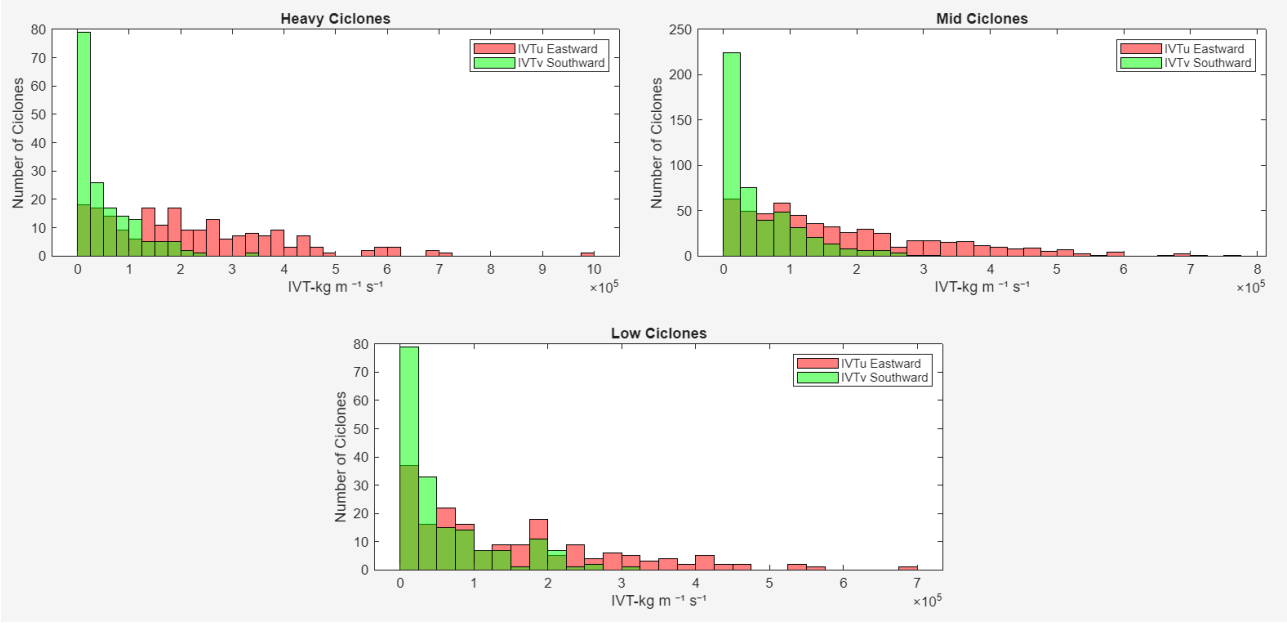

Figure 3.14- Histograms comparing the IVTu towards the East and the IVTv towards South for the three cyclone classes.

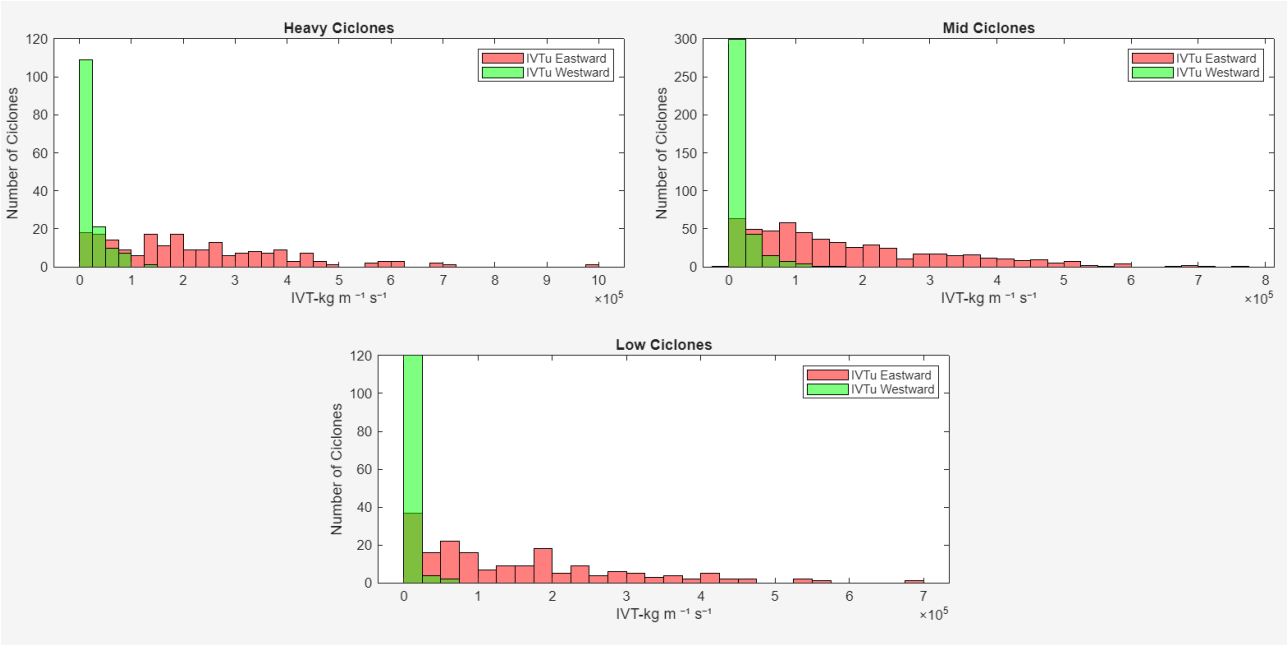

Figure 3.15- Histograms comparing the IVTu towards the East and the IVTu towards West for the three cyclone classes.

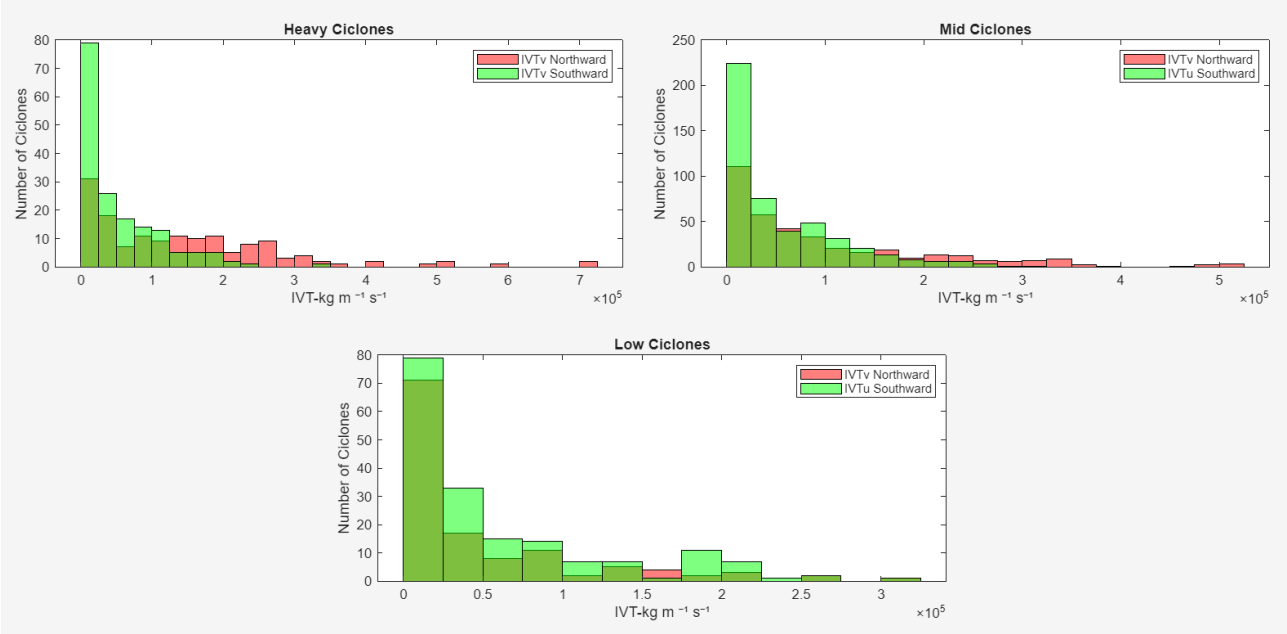

Figure 3.16- Histograms comparing the IVTv towards the North and the IVTv towards South for the three cyclone classes

The other variable investigated was the area of maximum extension. The results obtained are like those obtained for the IVT module and its components (some tables are found in Appendix C).
The analysis was also conducted for two, three and four days, the last of which was the initial day of the cyclone. In these cases, too, the results are essentially consistent with what was discussed above (some tables are provided in the Appendix C).

Chapter 4

Conclusions

This work sought to investigate the possible influence of moisture transport on the intrinsic predictability of extratropical cyclones in the eastern Mediterranean basin. Recent developments in dynamical systems theory have made it possible to characterise instantaneous atmospheric states using local properties of dynamical systems. Two metrics are particularly useful for describing a dynamic state locally: the local dimension d, which measures the number of degrees of freedom around a given atmospheric state and indicates how the system will evolve in the vicinity of that state, and the persistence θ^{-1} which quantifies, in phase space, the residence time of a trajectory of the system near that state. The combination of these two measures allows information to be acquired on the intrinsic local predictability of the atmosphere.
The values of the metrics d and θ for the eastern Mediterranean for a 38-year period, for various geopotential heights and for precipitation, were provided as input data.

Moisture transport was quantified using a vector quantity called Integrated Vapor Transport (IVT): defined as the horizontal advection of vapor integrated vertically along the vertical tropospheric column. To quantify the IVT vector, its zonal component IVTu and its meridional component IVTv were downloaded from the ERA5 database.

The data required to perform the analysis was completed by providing an additional list containing all cyclones that occurred during the period and in the area under consideration. In this list, the cyclones were classified into three groups (low, mid, heavy) according to their intensity.

We could not find any element suggesting the existence of a monotonic relationship between the increase in horizontal moisture flow, represented by the IVT vector module, and the inverse persistence θ. On the contrary, for metric d, the analysis showed consistent negative correlation between the local dimension d of the geopotential height Z1000 and of precipitation and IVT, which are statistically significant for the geopotential height Z1000 of mid- and heavy-intensity cyclone. This result suggests a possible monotonically decreasing relationship between the increase in horizontal moisture advection and the local dimension d, limited to the geopotential height Z1000 and mid- and heavy-intensity cyclones.
The most significant component was found to be the eastward component of the IVTu. In fact, the correlations obtained by placing it on the x-axis match the results previously obtained for the integral value of the modulus.

The results obtained using the area of maximum extension instead of the maximum integrated IVT are practically the same, both in the case of the IVT module and its components.

The use of tables has made it possible to represent the values of Pearson's and Spearman's correlation coefficients immediately. In a single table, the correlation values of 21 scatter plots can be viewed for a single day or for several days. This allows us to determine, in the case of Pearson, whether there is a possible linear relationship between the variables, and in the case of Spearman, whether there is a

possible monotonic relationship between the variables. But it cannot tell us anything about the possible existence of a relationship between variables that is not monotonic.
A further observation is that for each day, or series of days, we had several values of the maximum area or maximum integrated IVT available. To represent moisture transport, we chose the highest value. In this way, it is conceivable that we may not be able to fully capture the temporal evolution of a cyclone. We have taken a photograph that immortalises a moment in time, while an atmospheric phenomenon such as a cyclone also has a duration.

Several studies have investigated how increased humidity, sea level pressure, etc., influence intrinsic predictability, a working hypothesis could be to study moisture transport together with these other variables. Also, if the assumption made when considering a period of many years and focusing on the extreme values of a quantity, in our case the IVT, is that the other quantities involved tend to cancel out their influence.

The results of this study suggest that vapor transport could influence the intrinsic predictability of Mediterranean cyclones in the eastern portion of the basin. Intrinsic predictability is described using two metrics: local size d and the inverse of persistence θ. Moisture transport was quantified using the IVT vector. Analysis of its module suggested that an increase in moisture transport could lead to a decrease in the value of the local dimension d, and therefore to greater intrinsic predictability. However, this result is limited to the geopotential height Z1000 and to mid- and heavy-intensity cyclones. The separate analysis of the various components of the IVT yielded results consistent with those obtained for the module, except for the southern component of the IVT. In this case, an increase in moisture transport towards the south seems to result in an increase in the value of the local dimension d. This suggests the possibility of a decrease in intrinsic predictability.

Appendix A-Rotating System

Let us begin by considering a rotation A of the coordinate system K with respect to a fixed coordinate system k We will denote by $R(t)$ belonging to K the radius vector of a point moving in the moving coordinate system, and by $r(t) = AR(t)$ the radius vector of the fixed system. The angular velocity vector will be denoted by Ω in K system. Suppose that in the coordinate system k, the motion of point $r(t)$ is the solution to Newton's equation $m\ddot{r} = f(r, \dot{r})$.

The velocity seen in reference system k can be written as:

$$\dot{r} = A\dot{R} + \dot{A}R = A\dot{R} + \dot{A}A^{-1}r = A\dot{R} + Br \qquad \text{(A.1)}$$

Where we have defined the linear operator $B = \dot{A}A^{-1}$, which we prove to be a skew-symmetric operator. Therefore, we will have that the sum of B and its transpose B^t will be zero: $B + B^t = 0$

Proof. Given that operator A is an orthogonal operator from one Euclidean space to another , its transpose is its inverse $A^t = A^{-1}$. By differentiating the relationship $AA^t = I$ with respect to t, we get

$$A\dot{A}^t + \dot{A}A^t = 0 \quad \Longrightarrow \quad \left(\dot{A}\,A^{-1}\right)^t + \dot{A}A^{-1} = 0 \qquad \square$$

Lemma: Every skew-symmetric operator in three-dimensional oriented Euclidean space is a vector product operator for a fixed vector

$$Br = [\omega, r] \qquad \forall\, r \in \mathbb{R}^3$$

Proof: All skew-symmetric operators form $R^3 \longrightarrow \mathbb{R}^3$ form a linear space. Its dimension is 3, since a 3x3 skew-symmetric matrix is defined by the three elements that lie on one side of the diagonal.

The operator of vector multiplication by ω is linear and skew symmetric. The operator of vector multiplication for any vector in the three-dimensional space ω form a linear subspace of all antisymmetric operators.

The dimension of this subspace is 3. Therefore, the subspace of the vector multiplication is the space of all skew-symmetric operators. $\square$

In cartesian coordinates the operator B is given by an antisymmetric matrix; we denote its elements by $\pm\omega_{1,2,3}$

$$B = \begin{Vmatrix} 0 & -\omega_3 & \omega_2 \\ \omega_3 & 0 & -\omega_1 \\ -\omega_2 & \omega_1 & 0 \end{Vmatrix}$$

In this notation the vector $\omega = \sum_{i=1}^{3} \omega_i\, \boldsymbol{e_i}$ will be an eigen vector with eigenvalue 0. By applying B to the vector $r = \sum_{i=1}^{3} r_i\, \boldsymbol{e_i}$ we obtain by a direct calculation $Br = [\omega, r]$.

So, we can write (A.1):

$$\dot{r} = A\dot{R} + Br = A\dot{R} + [\omega, r] = A\dot{R} + [A\Omega, AR] = A(\dot{R} + [\Omega, R]) \qquad \text{(A.2)}$$

$[A\Omega, AR]$ is equal to $A[\Omega, R]$ since operator B preserves and orientation, and therefore the metric product.

Theorem: Motion in rotating system takes place as if three additional forces acted on every moving point $R(t)$ of mass m:

1. The inertial force of rotation: $m\left[\dot{\boldsymbol{\Omega}}, \boldsymbol{R}\right]$
2. The Coriolis force: $2m\left[\boldsymbol{\Omega}, \dot{\boldsymbol{R}}\right]$
3. The centrifugal force: $m\left[\boldsymbol{\Omega}, [\boldsymbol{\Omega}, \boldsymbol{R}]\right]$

Thus $$m\ddot{R} = F - m\left[\dot{\Omega}, R\right] - 2m\left[\Omega, \dot{R}\right] - m\left[\Omega, [\Omega, R]\right] \quad , \qquad \text{(A.3)}$$

where $AF\left(R, \dot{R}\right) = f(AR, (\dot{AR})$

Proof: Since $r = AR$ we have already seen that $\dot{r} = A(\dot{R} + [\Omega, R])$. Differentiating once more, we obtain

$$\begin{aligned} \ddot{r} &= \dot{A}\left(\dot{R} + [\Omega, R]\right) + A(\ddot{R} + \left[\dot{\Omega}, R\right] + \left[\Omega, \dot{R}\right]) \\ &= A(\left[\Omega, \left(\dot{\Omega} + [\Omega, R]\right)\right] + \ddot{R} + \left[\dot{\Omega}, R\right] + \left[\Omega, \dot{R}\right]) \\ &= A(\ddot{R} + 2\left[\Omega, \dot{R}\right] + \left[\Omega, [\Omega, R]\right] + \left[\dot{\Omega}, R\right]) \end{aligned}$$ □

(We again used the relationship $\dot{A}X = A[\Omega, X]$ for any vector $X \epsilon K$; this time $X = \dot{R} + [\Omega, R]$)

Appendix B- Poincare's recurrence theorem

Let us consider an autonomous system of differential equations $\dot{\boldsymbol{x}} = \mathbf{F}(\boldsymbol{x})$ (2.3) and let $\boldsymbol{\phi}^t$ be the corresponding group of transformations,

$$\boldsymbol{\phi}^t(\boldsymbol{x}) = \boldsymbol{x} + \mathbf{F}(\boldsymbol{x})t + O(t^2) \qquad (t \longrightarrow 0) \tag{B.1}$$

Suppose S_0 be a region of phase space with volume $V(t_0)$. Then $V(t)$ will be the volume of a region S_t of phase space such that $S_t = \boldsymbol{\phi}^t S_0$. We will demonstrate that the relationship holds true:

$$\left.\frac{dV(t)}{dt}\right|_{t=t_0} = \int_{S_0} \nabla \cdot \mathbf{F} dx \qquad (dx = dx_1\, dx_2 \cdots dx_n) \tag{B.2}$$

<u>In fact.</u> For each t, the formula for changing variables in a multiple integral (Jacobian) give

$$V(t) = \int_{S_t} dy = \int_{S_0} \det\frac{\partial \phi^t(x)}{\partial x} dx \qquad (y = \boldsymbol{\phi}^t(x),\ y \in S_t |\ x \in S_0)$$

Using formula (2.5) to calculate $\partial \boldsymbol{\phi}^t(x)/\partial x$, we find that for $t \longrightarrow 0$: $\frac{\partial \phi^t(x)}{\partial x} = I + \frac{\partial F}{\partial x} t + O(t^2)$
Now applying a well-known algebraic fact: $\det(I + Bt) = I + t\ tr\ B + O(t^2)$ $(t \longrightarrow 0)$, where B is a matrix $B = (b_{ij})$ and $tr\ B$ is his trace ($tr\ B = \sum_{i=1}^{n} b_{ii}$). We have,

$\det\frac{\partial \phi^t(x)}{\partial x} = I + t\ tr\frac{\partial F}{\partial x} + O(t^2)$ but $tr\frac{\partial F}{\partial x} = \sum_{i=1}^{n}\frac{\partial F_i}{\partial x_i} = \nabla \cdot \mathbf{F}$. Therefore,

$$V(t) = \int_{S_0} (1 + t\,\nabla \cdot \mathbf{F} + O(t^2)\, dx \implies \left.\frac{dV(t)}{dt}\right|_{t=t_0} = \int_{S_0} \nabla \cdot \mathbf{F} dx$$

If $\nabla \cdot \mathbf{F} \equiv 0$, $dV/dt \equiv 0$.
For a Hamiltonian system, where $(\mathrm{q_i}, \mathrm{p_i})$ are position-momentum coordinates for $i = 1, 2, \ldots, n$ and H(q, p, t), is the Hamiltonian function, the equation of motion reads:

$$\dot{q}_i = \frac{\partial H}{\partial p_i} \qquad\qquad \dot{p}_i = -\frac{\partial H}{\partial q_i} \tag{B.3}$$

Therefore, for a Hamiltonian system we have

$$\nabla \cdot \mathbf{F} = \sum_{i=1}^{2n}\frac{\partial f_i}{\partial x_i} = \sum_{i=1}^{n}\left(\frac{\partial}{\partial q_i}\frac{\partial H}{\partial p_i} - \frac{\partial}{\partial p_i}\frac{\partial H}{\partial q_i}\right) \equiv 0 \tag{B.4}$$

This observation (B.4) proves Liouville's theorem.

<u>Liouville's theorem</u> : The phase flow of Hamilton's equation preserve volume: for any region D we have $volume\ of\ \boldsymbol{\phi}^t D = volume\ of D$.

Poincaré's recurrence theorem: Let ϕ a volume-preserving one to one mapping which maps a bounding region D of Euclidian space onto itself: $\phi D = D$.

Then in any neighbourhood U of any point of D there is a point $x \in U$ which returns to U,i.e., $\phi^n x \in U$ for some $n > 0$.

In fact: We consider the image of the neighbourhood U: $U, \phi U, \phi^2 U, \ldots\ldots, \phi^n U$. All of these have the same volume. If they never intersect, D would have infinite volume. Therefore, for some $k \geq 0$ and $l \geq 0$, with $k > l$, $\phi^k U \cap \phi^l U \neq \emptyset$.

Therefore, $\phi^{k-l} U \cap U \neq \emptyset$. If y is in the intersection, then $y = \phi^n x$, with $x \in U$ $(n = k - l)$. □

This is one of the few general results on the nature of motion. A rather paradoxical consequence of Poincaré and Liouville's theorems is the following: if we open a partition separating a chamber filled with gas from an empty chamber, after a certain amount of time the gas molecules will gather again in the first chamber. The solution to the paradox lies in the fact that this "certain amount of time" is greater than the lifetime of the solar system

Appendix C-Tables

Some tables concerning the calculated correlation values are shown here. They are not included in the text but are referred to therein.

	metrics d, Maximum integrated vector IVT magnitude(Day the Cyclone plus 2 days before)					
	Low CL		Mid CL		heavy CL	
	r	ρ	r	ρ	r	ρ
Z=1000	-0.0583	-0.0993	-0.3140	-0.3639	-0.3445	-0.3830
Z=850	0.1259	0.1165	-0.0187	-0.0156	0.0078	-0.0645
Z=700	0.1823	0.1649	0.0868	0.0586	0.1301	0.1519
Z=500	0.0492	-0.0082	0.0172	0.0343	0.0906	0.0832
Z=300	0.1151	0.0694	0.1126	0.1111	0.2750	0.2145
Z=200	-0.0874	-0.1527	0.0014	-0.0140	-0.0984	-0.1168
Prec.	-0.1044	-0.1237	-0.2440	-0.2799	-0.1098	-0.1830

	metrics d, Maximum integrated vector IVT magnitude(Day the Cyclone plus 3 days before)					
	Low CL		Mid CL		heavy CL	
	r	ρ	r	ρ	r	ρ
Z=1000	-0.0382	-0.0898	-0.2774	-0.3404	-0.3407	-0.3859
Z=850	0.0741	0.0689	-0.0016	-0.0049	-0.0041	-0.0875
Z=700	0.1411	0.1101	0.1121	0.0768	0.1192	0.1319
Z=500	0.0104	-0.0661	0.0390	0.0390	0.0626	0.0458
Z=300	0.0740	0.0261	0.1513	0.1461	0.2427	0.1700
Z=200	-0.1058	-0.1668	-0.0104	-0.0402	-0.0784	-0.0861
Prec.	-0.0622	-0.0581	-0.2300	-0.2453	-0.1191	-0.1877

	metrics d, Maximum integrated vector IVT magnitude(Day the Cyclone plus 4 days before)					
	Low CL		Mid CL		heavy CL	
	r	ρ	r	ρ	r	ρ
Z=1000	-0.0418	-0.0794	-0.2524	-0.3019	-0.3381	-0.3937
Z=850	0.0811	0.0800	0.0060	0.0062	-0.0348	-0.1009
Z=700	0.1371	0.1120	0.1324	0.0987	0.1073	0.1255
Z=500	-0.0223	-0.0970	0.0532	0.0445	0.0593	0.0522
Z=300	0.0553	0.0076	0.1548	0.1525	0.2388	0.1723
Z=200	-0.1010	-0.1620	-0.0066	-0.0375	-0.0707	-0.0866
Prec.	-0.0688	-0.0621	-0.2295	-0.2404	-0.0898	-0.1663

	metrics d,Day before the cyclon, Maximum integrated zonal component IVT (IVTu Eastward)					
	Low CL		Mid CL		heavy CL	
	r	ρ	r	ρ	r	ρ
Z=1000	0.0135	-0.0352	-0.2511	-0.3135	-0.3048	-0.3653
Z=850	0.0344	0.0159	-0.0738	-0.0901	-0.0976	-0.1990
Z=700	0.0804	0.0947	0.0640	0.0318	0.0641	0.0250
Z=500	-0.0474	-0.0849	-0.0378	-0.0103	-0.0775	-0.0631
Z=300	0.0451	0.0032	0.0496	0.0564	-0.0048	-0.0278
Z=200	-0.0278	-0.1196	0.0423	0.0179	-0.0575	-0.1116
Prec.	-0.0753	-0.0691	-0.1442	-0.1690	-0.0675	-0.2120

	metrics d,Day before the cyclon, Maximum integrated meridional component IVT (IVTv Northward)					
	Low CL		Mid CL		heavy CL	
	r	ρ	r	ρ	r	ρ
Z=1000	-0.2270	-0.2197	-0.2722	-0.3380	-0.2759	-0.2464
Z=850	-0.1029	-0.1164	-0.0913	-0.0553	-0.0345	-0.0288
Z=700	0.1307	0.0985	0.0752	0.0680	0.1003	0.1387
Z=500	0.0455	-0.0585	0.0281	0.0404	0.1287	0.0685
Z=300	0.0739	0.0385	0.0455	0.0416	0.2169	0.2065
Z=200	-0.1410	-0.1836	-0.0210	-0.0377	-0.0018	-0.0478
Prec.	-0.0877	-0.2233	-0.1023	-0.0951	-0.1383	-0.1567

	metrics d,Day before the cyclon, Maximum integrated meridional component IVT (IVTv Southward)					
	Low CL		Mid CL		heavy CL	
	r	ρ	r	ρ	r	ρ
Z=1000	0.1155	0.0973	0.1099	0.1367	0.2752	0.3055
Z=850	0.2318	0.1377	0.1249	0.0487	0.2374	0.1264
Z=700	0.2203	0.0725	0.1605	0.0367	0.3106	0.1958
Z=500	0.2551	0.1336	0.1318	0.0988	0.1368	0.2012
Z=300	0.2207	0.1476	0.1871	0.1061	0.1170	0.1047
Z=200	0.2333	0.2784	0.1167	0.1314	-0.0007	0.0552
Prec.	-0.0485	0.0678	-0.0946	-0.0858	0.0392	0.0354

	metrics d, Maximum integrated IVTu (Eastward)(Day the Cyclone plus 2 days before)					
	Low CL		Mid CL		heavy CL	
	r	ρ	r	ρ	r	ρ
Z=1000	-0.0247	-0.0771	-0.3253	-0.3864	-0.3757	-0.4222
Z=850	0.1414	0.1267	-0.0257	-0.0278	-0.0843	-0.1953
Z=700	0.1236	0.1404	0.0453	0.0237	0.0152	-0.0268
Z=500	-0.0175	-0.0316	-0.0382	-0.0347	-0.0486	-0.0708
Z=300	0.0678	0.0452	0.0777	0.0658	0.1238	0.0641
Z=200	-0.0471	-0.1411	0.0157	-0.0052	-0.0778	-0.1103
Prec.	-0.0740	-0.1148	-0.2712	-0.3078	-0.1092	-0.2229

	metrics θ, Maximum integrated IVTu (Eastward)(Day the Cyclone plus 2 days before)					
	Low CL		Mid CL		heavy CL	
	r	ρ	r	ρ	r	ρ
Z=1000	-0.1382	-0.0845	0.0487	0.1045	-0.3253	-0.3864
Z=850	-0.0063	-0.0248	0.0078	0.0070	-0.0257	-0.0278
Z=700	-0.1042	-0.0270	0.0296	0.0561	0.0453	0.0237
Z=500	-0.1147	-0.0647	0.0414	0.0558	-0.0382	-0.0347
Z=300	-0.0694	-0.0147	0.1008	0.0809	0.0777	0.0658
Z=200	-0.0479	-0.0053	0.0734	0.0328	0.0157	-0.0052
Prec.	0.1482	0.1065	-0.0307	-0.0969	-0.2712	-0.3078

	metrics d, Maximum integrated IVTv (Southward)(Day the Cyclone plus 2 days before)					
	Low CL		Mid CL		heavy CL	
	r	ρ	r	ρ	r	ρ
Z=1000	0.1562	0.1666	0.2145	0.2007	0.4017	0.3057
Z=850	0.2759	0.2112	0.1878	0.1103	0.1134	0.0768
Z=700	0.2332	0.1061	0.2390	0.1597	0.2116	0.1344
Z=500	0.2142	0.1064	0.2985	0.2513	0.1771	0.1187
Z=300	0.2089	0.1641	0.2476	0.1957	0.0708	-0.0118
Z=200	0.2833	0.2954	0.0389	0.0072	-0.0063	-0.0291
Prec.	-0.0635	-0.0254	-0.0463	-0.0274	0.0298	0.0272

	metrics d, Maximum integrated IVTv (Northward)(Day the Cyclone plus 2 days before)					
	Low CL		Mid CL		heavy CL	
	r	ρ	r	ρ	r	ρ
Z=1000	-0.1902	-0.1443	-0.2832	-0.3418	-0.3296	-0.3319
Z=850	-0.0524	-0.0553	-0.0386	-0.0060	0.0400	0.0386
Z=700	0.1281	0.1216	0.0481	0.0384	0.1298	0.2006
Z=500	0.0267	-0.0008	0.0146	0.0227	0.1561	0.1119
Z=300	0.0496	0.0288	0.0693	0.0729	0.3618	0.3127
Z=200	-0.2286	-0.2595	-0.0231	-0.0451	-0.0424	-0.0865
Prec.	-0.0932	-0.1965	-0.1475	-0.1482	-0.1323	-0.1298

	metrics θ, Maximum integrated IVTv (Northward)(Day the Cyclone plus 2 days before)					
	Low CL		Mid CL		heavy CL	
	r	ρ	r	ρ	r	ρ
Z=1000	-0.0668	0.0301	0.0246	0.0707	-0.2832	-0.3418
Z=850	-0.2177	-0.1714	-0.0793	-0.0457	-0.0386	-0.0060
Z=700	-0.2091	-0.1649	-0.0599	-0.0552	0.0481	0.0384
Z=500	-0.1606	-0.0801	0.0332	0.0144	0.0146	0.0227
Z=300	-0.1384	-0.0538	0.1151	0.0797	0.0693	0.0729
Z=200	-0.1676	-0.0776	0.0064	-0.0201	-0.0231	-0.0451
Prec.	0.2184	0.1298	0.0996	0.0069	-0.1475	-0.1482

	metrics d, Maximum integrated IVTu (Eastward)(Day the Cyclone plus 3 days before)					
	Low CL		Mid CL		heavy CL	
	r	ρ	r	ρ	r	ρ
Z=1000	0.0036	-0.0504	-0.2989	-0.3605	-0.3618	-0.4063
Z=850	0.0948	0.0854	-0.0203	-0.0209	-0.0989	-0.2177
Z=700	0.0922	0.1114	0.0656	0.0485	0.0065	-0.0385
Z=500	-0.0428	-0.0633	-0.0111	-0.0221	-0.0702	-0.0992
Z=300	0.0356	0.0189	0.1210	0.0987	0.0836	0.0098
Z=200	-0.0557	-0.1366	0.0012	-0.0269	-0.0562	-0.0783
Prec.	-0.0623	-0.0674	-0.2448	-0.2682	-0.1224	-0.2417

	metrics d, Day the cyclon, Maximum Area					
	Low CL		Mid CL		heavy CL	
	r	ρ	r	ρ	r	ρ
Z=1000	-0.0392	-0.0828	-0.3217	-0.3601	-0.3772	-0.3863
Z=850	0.2726	0.2612	0.0073	0.0272	0.0014	-0.0127
Z=700	0.2177	0.1975	0.0846	0.0763	0.0819	0.1481
Z=500	0.1322	0.1305	0.0339	0.0544	0.0794	0.0954
Z=300	0.1455	0.1180	0.0976	0.1039	0.2573	0.2162
Z=200	0.0251	-0.0185	0.0002	-0.0144	-0.1529	-0.1590
Prec.	-0.0228	-0.1137	-0.2779	-0.2868	-0.1956	-0.1881

	metrics d,Day before the cyclon, Maximum Area					
	Low CL		Mid CL		heavy CL	
	r	ρ	r	ρ	r	ρ
Z=1000	-0.0376	-0.0479	-0.2881	-0.3314	-0.3704	-0.3682
Z=850	0.0821	0.0591	-0.1116	-0.1130	-0.1085	-0.1378
Z=700	0.2178	0.1698	0.0784	0.0530	0.0543	0.0949
Z=500	0.0998	0.0099	-0.0140	0.0051	0.0022	0.0441
Z=300	0.1599	0.0827	0.0621	0.0665	0.0911	0.1174
Z=200	-0.0488	-0.1052	0.0307	0.0270	-0.0643	-0.0810
Prec.	-0.0780	-0.0457	-0.1508	-0.1705	-0.1714	-0.1927

	metrics θ, Day the cyclon, Maximum Area					
	Low CL		Mid CL		heavy CL	
	r	ρ	r	ρ	r	ρ
Z=1000	-0.2216	-0.1152	0.0267	0.0920	-0.1804	-0.1110
Z=850	-0.0093	0.0511	-0.0330	-0.0187	-0.1519	-0.0925
Z=700	-0.1306	-0.0437	-0.0453	0.0036	-0.0161	0.0185
Z=500	-0.0820	-0.0672	0.0111	0.0204	0.1927	0.2125
Z=300	-0.0216	-0.0137	0.1248	0.0920	0.2108	0.2152
Z=200	0.0243	0.0207	0.0577	0.0305	0.1605	0.1151
Prec.	0.2979	0.2222	0.0469	-0.0167	-0.0058	-0.0866

	metrics d, Maximum Area(Day the Cyclone plus 2 days before)					
	Low CL		Mid CL		heavy CL	
	r	ρ	r	ρ	r	ρ
Z=1000	-0.0619	-0.1020	-0.3454	-0.3781	-0.3733	-0.3793
Z=850	0.1438	0.1081	-0.0427	-0.0351	-0.0688	-0.0800
Z=700	0.2032	0.1728	0.0678	0.0605	0.0755	0.1309
Z=500	0.0647	0.0076	0.0231	0.0411	0.0647	0.0681
Z=300	0.1118	0.0780	0.1111	0.1187	0.2349	0.1953
Z=200	-0.0814	-0.1567	-0.0026	-0.0138	-0.1226	-0.1279
Prec.	-0.0990	-0.1099	-0.2660	-0.2806	-0.1564	-0.1549

	metrics d, Day the cyclon, Maximum Area (IVTu Eastward)					
	Low CL		Mid CL		heavy CL	
	r	ρ	r	ρ	r	ρ
Z=1000	-0.0633	-0.1050	-0.3404	-0.3828	-0.4373	-0.4378
Z=850	0.2082	0.2096	-0.0415	-0.0099	-0.1412	-0.1669
Z=700	0.0858	0.1323	0.0300	0.0278	-0.0524	-0.0302
Z=500	0.0069	0.0590	-0.0631	-0.0464	-0.0510	-0.0725
Z=300	0.0680	0.0665	0.0127	0.0124	0.1169	0.0628
Z=200	-0.0426	-0.1110	0.0438	0.0325	-0.1046	-0.1227
Prec.	0.0034	-0.1311	-0.3222	-0.3355	-0.2283	-0.2357

	metrics d,Day before the cyclon, Maximum Area (IVTu Eastward)					
	Low CL		Mid CL		heavy CL	
	r	ρ	r	ρ	r	ρ
Z=1000	-0.0134	-0.0309	-0.2698	-0.3129	-0.3400	-0.3564
Z=850	0.0175	0.0065	-0.1038	-0.0997	-0.1568	-0.2152
Z=700	0.0826	0.0892	0.0342	0.0251	0.0202	0.0065
Z=500	-0.0499	-0.0912	-0.0424	-0.0174	-0.0873	-0.0783
Z=300	0.0376	0.0035	0.0346	0.0497	-0.0159	-0.0475
Z=200	-0.0436	-0.1231	0.0330	0.0182	-0.0758	-0.1054
Prec.	-0.0902	-0.0541	-0.1585	-0.1684	-0.1576	-0.1995

Percentiles $IVTu$ and $IVTv$

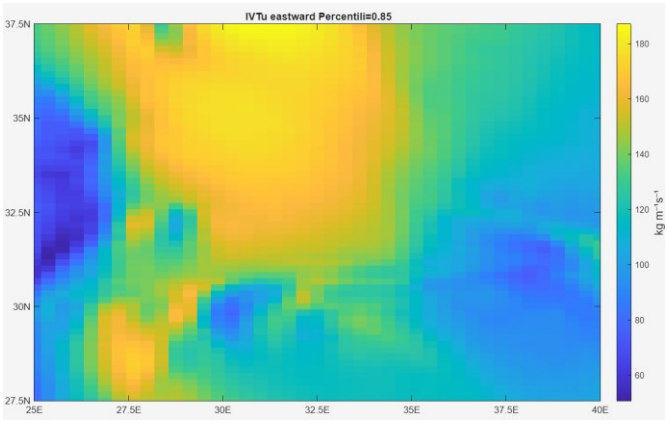

IVTu towards the East

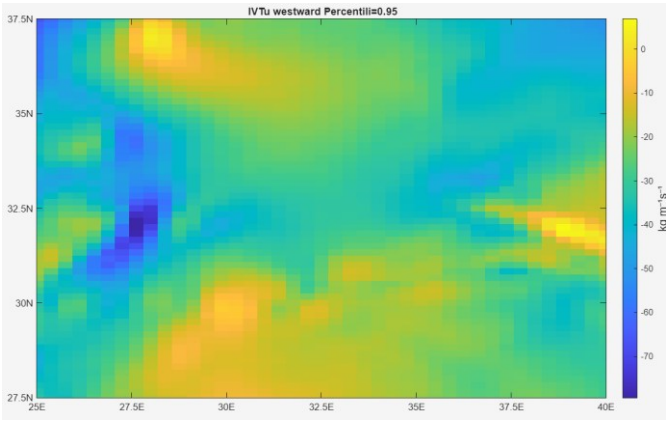

IVTu towards the West

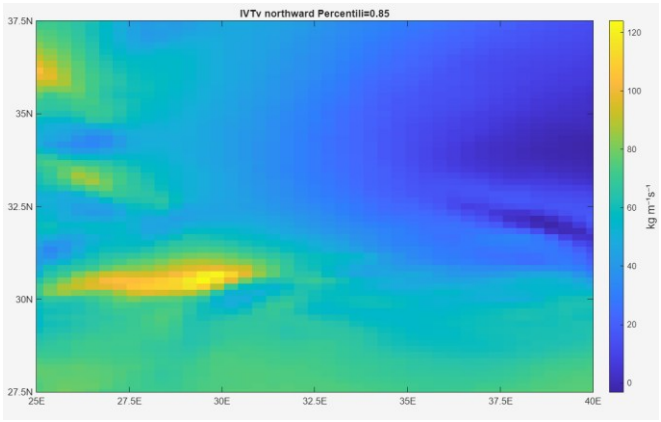

IVTv towards the North

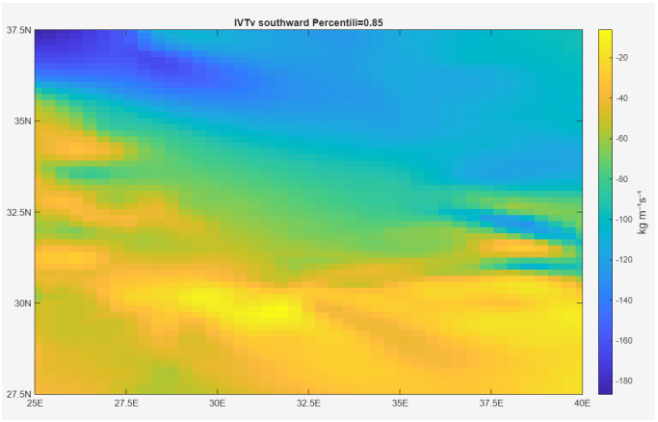

IVTv towards the South

	metrics d, Day the cyclon, -thresholds					
	Low CL		Mid CL		heavy CL	
	r	ρ	r	ρ	r	ρ
Z=1000	-0.1163	-0.1119	-0.0704	-0.0709	-0.1102	-0.1179
Z=850	0.1255	0.1192	0.0751	0.0757	0.1090	0.1110
Z=700	0.1219	0.1255	0.0757	0.0670	0.1105	0.1135
Z=500	0.1267	0.1241	0.0752	0.0721	0.1264	0.1236
Z=300	0.1249	0.1221	0.0737	0.0703	0.1129	0.1146
Z=200	0.1182	-0.1187	-0.0681	-0.0627	-0.1125	-0.1166
Prec.	-0.1015	-0.1186	-0.0711	-0.0674	-0.1153	-0.1138

	metrics d, Day before the cyclon, -thresholds					
	Low CL		Mid CL		heavy CL	
	r	ρ	r	ρ	r	ρ
Z=1000	-0.1141	-0.1192	-0.0639	-0.0698	-0.1065	-0.1153
Z=850	0.1178	0.1191	-0.0700	-0.0728	-0.1216	-0.1210
Z=700	0.1335	0.1210	0.0737	0.0673	0.1140	0.1099
Z=500	0.1254	-0.1243	-0.0716	0.0678	0.1254	0.1268
Z=300	0.1225	0.1262	0.0736	0.0693	0.1226	0.1167
Z=200	-0.1167	-0.1180	0.0711	0.0712	-0.1165	-0.1162
Prec.	-0.1035	-0.1165	-0.0709	-0.0703	-0.1213	-0.1134

Bibliography

Assaf Hochman, Tair Plotnik, Francesco Marra, Elizabeth-Ruth Shehter, Shira Raveh-Rubin, Leehi Magaritz-Ronen (2023).The sources of extreme precipitation predictability; the case of the 'Wet' Red Sea Trough. Weather and Climate Extremes. https://iris.cnr.it/retrieve/82a6e9a1-1cf6-4401-8427-af076bf79ed8/1-s2.0-S2212094723000178-main_compressed.pdf

Assaf Hochman, Sebastian Scher, Julian Quinting, Joaquim G. Pinto, Gabriele Messori (2020) Dynamics and predictability of cold spells over the Eastern Mediterranean. https://esd.copernicus.org/articles/12/133/2021/

Assaf Hochman, Tzvika Harpaz, Hadas Saaroni and Pinhas Alpert (2017). Synoptic classification in 21st century CMIP5 predictions over the Eastern Mediterranean with focus on cyclones. https://www.tau.ac.il/~pinhas/papers/2017/Hochman_et_al_IJC_2017a.pdf

Bassi Alberto (2022)- Reconstruction and Parameter Estimation of Dynamical Systems using Neural Networks-Final Dissertation. https://thesis.unipd.it/handle/20.500.12608/34718

Chenyu Dong, Davide Faranda, Adriano Gualsandi, Valerio Luccarini, Gianmarco Mengaldo (2024). Revisiting the predictability of dynamical systems: a new local data-driven approach. https://arxiv.org/html/2409.14865v1

Ciceri Riccardo (2024)-Thermodynamic and dynamic contributions to changes in extreme precipitation- Final Dissertation. https://thesis.unipd.it/handle/20.500.12608/80504

Davide Faranda, Gabriele Messori & Pascal Yiou (2017). Dynamical proxies of North Atlantic predictability and extremes, SCIENTIFIC REPORTS. https://www.nature.com/articles/srep41278

Edward Ott (2002). Chaos in Dynamical Systems. Cambridge University Press, 2 editions.

F.M. Ralph, S.F. Iacobellis, P. J. Neiman, J. M. Cordeira, J. R. Spackman, D.E. Waliser, G. A. Wick, A.B. White and C. Fairall (2017). Dropsonde Observations of Total Integrated Water Vapor Transport within North Pacific Atmospheric Rivers. https://cw3e.ucsd.edu/wp-content/uploads/2017/07/Ralphetal2017-JHMDropsondes.pdf

J.-P. Eckmann, D. Ruelle (1985)- Ergodic theory of chaos and strange attractors- The American Physics Society- Reviews of Modern Physics, Vol. 57,No. 3. https://www.ihes.fr/~ruelle/PUBLICATIONS/%5B81%5D.pdf

Loreti, Maurizio (1998). Teoria degli errori e fondamenti di statistica. Introduzione alla fisica sperimentale. Decibel Zanichelli.

Lucarini Valerio, Davide Faranda, Jorge Miguel Milhazes de Freitas, Mark Holand, Tobias Kuna, Matthew Nicol, Mike Todd, Sandro Vaienti, et al. Extremes and Recurrence in Dynamical Systems. Pure and Applied Mathematics: A Wiley Series of Texts, Monographs and Tracts (Wiley, 2016).

Lucarini V., Faranda, D. & Wouters, J. Universal behaviour of extreme value statistics for selected observables of dynamical systems . *Stat*. *Phys*. 147, 63–73 (2012). https://arxiv.org/abs/1110.0176

Mazzone Giorgio, Daniele Mirabile Gattia (2006). Appunti di Termodinamica dei Solidi. ENEA.

Pedro M. Sousa, Alexandre M. Ramos, Christoph C. Raible, M. Messmer, Riccardo Tomé, Joaquin G. Pinto, Riccardo M. Trigo (2019). North Atlantic Integrated Water Vapor Trasport-From 850 to 2100 CE: Impacts on Western European Rainfall. https://climatehomes.unibe.ch/~raible/Sousa_et_al-2020-JournalofClimate.pdf

Strogatz H. Steven (2015). Nonlinear Dynamics and Chaos. CRC Press, second edition.

Vladimir Igorevič Arnold (2010) - Metodi Matematici della Meccanica Classica. Editori Riuniti, University press.

Wallace, J.M. and P.V. Hobbs (2006). Atmospheric Science: An Introductory Survey. International Geophysics. Academic Press. isbn: 9780080499536.

Yang Peicai (1991). On the Chaotic Behaviour and Predictability of the Real Atmosphere. Advances in Atmospheric Sciences. Vol.8 No.4. https://link.springer.com/article/10.1007/BF02919264